

CALSPAN ADVANCED TECHNOLOGY CENTER BUFFALO NY AERODYN--ETC F/G 20/4
TRANSONIC SHOCK WAVE - BOUNDARY LAYER INTERACTIONS.(U)
MAY 80 C PADOVA, T J FALK F44620-76-C-0057
CALSPAN-AB-5866-A-4 AFOSR-TR-80-0694 NL

TRANSONIC SHOCK WAVE - BOUNDARY LAYER INTERACTIONS. (U)

MAY 80 C PADOVA, T J FALK

F44620-76-C-0057

UNCLASSIFIED

CALSPAN-AB-5866-A-4

AFOSR-TR-80-0694

NL

1 of 1
AQ A
048821

AD A
048821

END

DATE _____

FILMED

68

DTIC

AEOSR-TR- 80-0694

LEVEL

12
P.S.

CALSPAN ADVANCED TECHNOLOGY CENTER

AD A088831

TRANSONIC SHOCK WAVE - BOUNDARY LAYER INTERACTIONS

C. Padova and Theodore J. Falk
Aerodynamic Research Department

Calspan Report No. AB-5866-A-4
May 1980

Contract No. F44620-76-C-0057
Final Report

DTIC
SELECTED
SEP 4 1980

Prepared for:
AIR FORCE OFFICE OF SCIENTIFIC RESEARCH
BOLLING AIR FORCE BASE
WASHINGTON, DC 20332

Approved for public release;
distribution unlimited

A DIVISION OF CALSPAN CORPORATION

80 9 2 064

REPORT DOCUMENTATION PAGE		READ INSTRUCTIONS BEFORE COMPLETING FORM	
1. REPORT NUMBER (18) AFOSR-TR- 80-0694	2. GOVT ACCESSION NO. AD-A088832	3. RECIPIENT'S CATALOG NUMBER	
4. TITLE (and Subtitle) TRANSONIC SHOCK WAVE - BOUNDARY LAYER INTERACTIONS	5. TYPE OF REPORT & PERIOD COVERED (9) FINAL	1-7 Jan 70 - Apr 80	
6. AUTHOR(s) (10) CORSO/PADOVA, THEODORE J. FALK	7. PERFORMING ORG. REPORT NUMBER AB-5866-A-4	8. CONTRACT OR GRANT NUMBER(s) F44620-76-C-0057	
9. PERFORMING ORGANIZATION NAME AND ADDRESS CALSPAN CORPORATION, ADVANCED TECHNOLOGY CENTER P. O. BOX 400 BUFFALO, NY 14225	10. PROGRAM ELEMENT, PROJECT, TASK AREA & WORK UNIT NUMBERS (16) 2307A1 61102F	(17) A1	
11. CONTROLLING OFFICE NAME AND ADDRESS AIR FORCE OFFICE OF SCIENTIFIC RESEARCH/NA BLDG 410 BOLLING AIR FORCE BASE, DC 20332	12. REPORT DATE May 1980	13. NUMBER OF PAGES 94	
14. MONITORING AGENCY NAME & ADDRESS (if different from Controlling Office) (14) CAL-PAI-AE-5866-A-4	15. SECURITY CLASS. (of this report) UNCLASSIFIED		
15a. DECLASSIFICATION/DOWNGRADING SCHEDULE			
16. DISTRIBUTION STATEMENT (of this Report) Approved for public release; distribution unlimited			
17. DISTRIBUTION STATEMENT (of abstract entered in Block 20, if different from Report)			
18. SUPPLEMENTARY NOTES			
19. KEY WORDS (Continue on reverse side if necessary and identify by block number) REYNOLDS NUMBER INTERACTING SHOCK WAVE TURBULENT BOUNDARY LAYER TRANSONIC SHOCK WAVE TRANSONIC SPEEDS SHOCK-INDUCED BOUNDARY LAYER SEPARATION			
20. ABSTRACT (Continue on reverse side if necessary and identify by block number) A series of 20 experiments was performed in a large-scale Ludwig tube to investigate the interactions of a normal shock with a turbulent boundary layer at unit Reynolds numbers 14.8×10^6 and 29.5×10^6 m and Mach numbers 1.43 and 1.60. In addition, the effects of a diverging flow field downstream of the shock, such as that which might be encountered on an airfoil, were explored by testing with a shock holder having a perforated top wall. The latter experiments were performed at the two Reynolds number values of 9 million and 36 million.			

DD FORM 1 JAN 73 1473

UNCLASSIFIED
SECURITY CLASSIFICATION OF THIS PAGE (When Data Entered)

391214

UNCLASSIFIED

million.

The results show that unit Re variations affected the interacting flow only by changing the boundary layer entering the interaction. The surface pressure distribution normalized by the thickness of the incoming boundary layer, which was measured in each experiment, describes an interaction independent of unit Re . In contrast, the interaction flow field was found to be very dependent on Mach number and on constraint of the subsonic region. In fact, shock configuration, surface pressure, skin friction and velocity profiles were found much more sensitive to these parameters than to the Reynolds number, which was investigated in earlier studies.

The bifurcation height and the length of separated flow increased with increasing M . Both quantities responded dramatically to the moderate but sustained flow deflections imposed by the perforated shock holders. The initial rise in surface pressure was found to correlate directly with the height of the bifurcated shock structure. However, the coupling of the surface pressure distribution with the shock structure dies out quickly in the displacement phase of the boundary layer development. At some distance from the shock system, the results indicate a marked hierarchy in the dependence of the subsonic pressure and the velocity fields on the subsonic boundary conditions. Correspondingly, inferences on shock-boundary layer interactions based on surface pressure measurements only, which are frequently drawn in airfoil work, appear questionable.

UNCLASSIFIED

SECURITY CLASSIFICATION OF THIS PAGE (When Data Entered)

PREFACE

This report describes the work performed by Calspan ATC for the Air Force Office of Scientific Research under Contract No. F44620-76-C-0057. The investigation was conducted in the Aerodynamic Research Department of the Calspan Advanced Technology Center, Buffalo, New York between January 76 and April 80. Technical Representatives for the Air Force were Mr. Milton Rogers and Dr. James Wilson.

The research reported here was initiated by Mr. Robert J. Vidal. To the sorrow of all of his friends at Calspan and elsewhere, Mr. Vidal died suddenly in May 1978. The work was continued by Theodore J. Falk and Corso Padova, with Dr. Falk serving as principal investigator.

AIR FORCE OFFICE OF SCIENTIFIC RESEARCH (AFSC)

NOTICE OF TRANSMITTAL TO DDC

This technical report has been reviewed and is approved for public release IAW AFR 190-12 (7b). Distribution is unlimited.

A. D. BLOOM

Technical Information Officer

TABLE OF CONTENTS

<u>Section</u>	<u>Page</u>
1. INTRODUCTION	1
2. EXPERIMENT	6
2.1 Calspan Ludwig Tube	6
2.2 The Simulation Experiment.....	8
2.3 Validity of the Experiment	11
2.4 Model and Instrumentation	14
2.5 Data Reduction	26
3. RESULTS	31
3.1 Review of Re_L Effect in Area Relief Model ..	31
3.2 Summary of Mach Number Effects	40
3.3 Summary of Unit Re Investigation	41
3.4 Summary of T_w/T_o Effects	42
3.5 Effects of Variations in Subsonic Boundary Geometry	44
3.6 Re_L Effect in Porous Shock Holder	62
3.7 Additional Data for a Baseline Interaction.	65
4. COMPARISON WITH OTHER EXPERIMENTS	72
5. CONCLUSIONS	80
REFERENCES	83

Accession for	
NTIS Global	
DOC TAB	
Unannounced	
Justification	
By	
Distribution	
Availability Codes	
Available/or	
Dist	special
A	

LIST OF FIGURES

FIGURE		PAGE
1	Calspan Ludwig Tube and Schematic of Model Installation..	7
2	Comparison of Local Mach Number Distribution in Flight and in Ludwig Tube	12
3	Spanwise Distribution of Static Pressure, $Re_L = 9 \times 10^6$, $x_3/\delta_u = 0.83$	13
4	Test Apparatus	15
5	Modified Test Apparatus	17
6	Shock Holder Configurations	18
7	Typical Pitot-Static Rakes	21
8	Skin Friction - Surface Pressure Survey Plate	22
9	Rake Spanning Full Model Height	24
10	Floor Pressure Tap Locations	25
11	Flow Angle Probe and Transducer	27
12	Effect of Re_L on Shock Structure	33
13	Generalized Wall Pressure	36
14	Shock-Free Wall Pressure and Friction	46
15	Undisturbed Velocity Profiles	47
16	Observed Shock Structures, 9.4% Linearly Tapered Porosity .	51
17	Location of Bifurcation Point, $M = 1.43$, $Re_L = 36 \times 10^6$...	53
18	Effect of Subsonic Boundary Variation on Wall Pressure, $Re_L = 36 \times 10^6$	57
19	Comparison of Velocity Profiles	60
20	Location of Bifurcation Point, $M = 1.43$, $Re_L = 9 \times 10^6$	63

LIST OF FIGURES (Cont'd.)

<u>FIGURE</u>		<u>PAGE</u>
21	Effect of Subsonic Boundary Variations on Wall Pressure, $Re_L = 9 \times 10^6$	64
22	Streamline Angles at 9.4LT Shock Holder, $Re_L = 36 \times 10^6$	67
23	Skin Friction Distribution	68
24	Velocity Profiles at 1 and 20 δ_u	70
25	Comparison of Bifurcation Heights in Nearly Unconstrained Interactions	73
26	Comparison of Bifurcation Heights in Constrained Interactions	75
27	Comparison of Separation Length Measurements.....	79

LIST OF SYMBOLS

A	cross-sectional area
b	span of shock holder channel
c	airfoil chord length
C_1, C_2	empirical constants in Eq. 1.
C_f	skin friction coefficient (referenced to sonic conditions)
d_λ	distance of the shock bifurcation point from the model lip
h	height of the test flow
h_c	open height of shock holder exit
H	boundary layer profile shape factor, δ^*/θ
L	length of flat plate
ℓ_s	length of separated flow region
M	Mach number
n	exponent in velocity profile power law representation, $\frac{u}{u_\delta} = \left(\frac{y}{\delta} \right)^{1/n}$
p	pressure
q	dynamic pressure
r	local pressure recovery relative to the expected normal shock value, $[P/P_\infty]/[P/P_o]$ normal shock
Re_L, Re_{δ_u}	Reynolds number based on plate length and undisturbed boundary layer thickness, respectively
T	temperature
u	streamwise velocity
W	mass flow rate per unit area
x	streamwise distance from shock wave
X	streamwise coordinate, in model frame of reference
y	normal coordinate
z	spanwise coordinate
α	streamline angle in pitch plane
δ	boundary layer thickness
δ^*	displacement thickness

LIST OF SYMBOLS (cont'd.)

θ	momentum thickness
λ	height of bifurcated shock wave
σ	ratio of open-to-closed area in perforated shock holder.

SUBSCRIPTS AND SUPERSSCRIPTS

0	at stagnation
i	charge conditions in Ludwig Tube supply.
k	at location of kink in surface pressure distribution
l	at the shock holder lip
s	at the shock location (does not apply to \mathcal{L}_s)
u	in the undisturbed flow ahead of the interaction
w	at the wall
δ	at the edge of the boundary layer
λ	at the bifurcation point
*	critical flow conditions ($M = 1$); does not apply to δ^* .

LIST OF TABLES

<u>TABLE</u>		<u>PAGE</u>
I	Undisturbed Boundary Layer Parameters (Area Relief Holder Experiments).....	32
II	Re_L Effect on Wall Pressure Parameters	36
III	Undisturbed Boundary Layer Parameters (Perforated Holder Experiments)	45
IV	Character of the Shock Structure Observed When Changing Porosity/Choke Settings	49
V	Extent of the Interaction Vs. Shock Position	54
VI	Wall Pressure Parameters Vs. Shock Position	58

Section 1

INTRODUCTION

Scaling of transonic wind tunnel data to full scale conditions when a shock wave-turbulent boundary layer interaction is imbedded in the flow remains one of the important unsolved problems in aerodynamic applications. In the late sixties, the conventional technique of simulating Mach number in the overall flow and compensating for full scale Reynolds number (Re_L) effects on the viscous layer by producing artificially early transition were found to have serious shortcomings^{1,2}. It was found that in aircraft configurations both the position of the supercritical shock wave on the wing and the chordwise extent of the shock-induced separation, changed substantially between the wind tunnel conditions and the flight conditions. These changes, in turn, produced significant effects on the airplane load distribution. These observations led to a research program at Calspan to investigate shock wave-boundary layer interactions.

This research program, the various phases of which have been sponsored by ONR*, AFOSR** and NAVAIR*** has investigated the influence of Reynolds number, unit Reynolds number, Mach number, wall-to-total temperature ratio and subsonic boundary geometry on the shock wave-boundary layer inter-

*Office of Naval Research Contract Nos. N00014-71-C-016 and N00014-76-C-0630.

**U.S. Air Force Office of Scientific Research Contracts Nos. F44620-71C-0046 and F44620-76C-0057.

***Naval Air Systems Command Contracts Nos. N00019-75-C-0433 and N00019-77-C-0179.

1. Loving, D.L., "Wind-Tunnel-Flight Correlation of Shock-Induced Separated Flows," NASA-TN-D-3850, September 1966.
2. Pearcey, H.H., Osborne, J. and Haines, A.B., "The Interaction Between Local Effects at the Shock and Rear Separation - A Source of Significant Scale Effects in Wind-Tunnel Tests on Aerofoils and Wings," AGARD Conference Proceedings No. 35, Paper No. 11, 1968.

action. The research has provided the first description³ of the important influence of Reynolds number on the interaction directly applicable to the problem of Ref. 1. With its extension⁴ to other governing parameters, the research has generated a data base which provides a description of the phenomena which result from changes in the parameters considered. The local picture of the flow field thus obtained may be patched into a larger description of the flow field in the vicinity of an airfoil, or the data may be used to anchor the theoretical codes which are now becoming capable of attacking the same interaction problem.

The original purpose of the AFOSR-sponsored research was to attempt to explain the results cited in Ref. 1 and, consequently, it centered on investigating the influence of Reynolds number on the interaction between a shock wave and a turbulent boundary layer at transonic speeds. A simulation experiment was designed and performed in a large-scale Ludwig tube in which an airfoil pressure distribution, with an interacting shock wave, was impressed upon a flat plate. The details of the interaction between the shock wave and the turbulent boundary layer were studied by measurements of surface pressure and skin friction, by pitot-static pressure measurements, and by schlieren observations with a high speed framing camera. Experiments were performed at Reynolds numbers, based on shock position, ranging from 9 million to 72 million. It was found that there were important Reynolds number effects on both the crosswise and the streamwise extent of the interaction. In particular, with a fourfold increase of Re_L from 9×10^6 to 36×10^6 , the length of shock-induced separation was found to decrease

3. Vidal, R.J., Wittliff, C.E., Catlin, P.A. and Sheen, B.H., "Reynolds Number Effects on the Shock Wave-Turbulent Boundary-Layer Interaction at Transonic Speeds," AIAA Paper No. 73-661, AIAA 6th Fluid and Plasma Dynamic Conference, Palm Springs, CA., 16-18 July 1973.
4. Padova, C., Falk, T.J. and Wittliff, C.E., "Experimental Investigation of Similitude Parameters Governing Transonic Shock-Boundary Layer Interactions," AIAA Paper No. 80-0158, AIAA 8th Aerospace Sciences Meeting, Pasadena, CA, 14-16 January 1980.

nearly fourfold. Concurrently, however, the Calspan experiments revealed that study of the influence of additional parameters affecting the interaction was required. In response, the research program was directed to explore the influence of unit Reynolds number, Mach number, wall-to-total temperature ratio and subsonic boundary geometry.

In the original apparatus, the Re_L had been varied from wind tunnel to full scale values by increasing the density of the test flow sweeping a model of fixed dimensions. The question of possible influence of unit Reynolds number changes on the separation characteristics of the interaction arose naturally. Influence of unit Re on viscous phenomena has been a concern for a decade. Furthermore, theoretical studies concurrent at the time of the early experiments indicated a possible unit Re effect on the transformation of the inner boundary layer region for near-separation velocity profiles. Ad hoc experiments were planned to study unit Re influence in Calspan's simulation of the interaction. These experiments repeated measurements at a Re_L , based on shock position, of 36×10^6 in a model with a flat plate of half the previous length. Doubling the density in the test flow maintained the desired Re_L in the reduced size model. The unit Re was thus increased by a factor of two as well.

In the initial set of Calspan experiments, a distinctive difference in the velocity transformation through the interaction was found relative to the classical measurements of Seddon and a Mach number effect was suspected to be the cause. Seddon observed a region of supersonic flow to remain just downstream of the bifurcated shock structure. Calspan measurements showed an overshoot in the speed of the stream, but no supersonic flow in the same interaction region. Since differences in Mach number were present between the two sets of experiments, one Re_L condition was repeated at higher M to investigate the influence of the latter parameter on the interaction process. A Mach number of approximately 1.6 was selected to this end and for its

applicability to maneuvering aircraft configurations as well.

Interest in the effects of heat transfer on the interaction arose, originally, from the fact that the Re_L investigation had been performed at a model-to-total temperature ratio (T_w/T_o) slightly above one. This temperature ratio value is characteristic of the Ludwig Tube Facility working with ambient temperature in the supply tube. Subsequent modifications of the Ludwig Tube allowed control of the total temperature in the test flow. Interactions with heat transfer from the flow to the model, or adiabatic conditions were then investigated. The results of this investigation appear very significant with respect to the effects of temperature non-equilibration on data measured in cryogenic tunnels such as the National Transonic Facility (NTF).

Finally, the effects on the interaction of changes forced in the subsonic flow region downstream the shock were investigated. Most existing data relating to the normal shock-boundary layer interaction problem have been measured under conditions intended to simulate the interaction occurring on a flat plate in an unconfined flow. However, the equivalent interaction on an airfoil is of great practical interest. In the airfoil case, the shock is commonly located in a region of adverse pressure gradient, which can be expected to delay recovery of the boundary layer weakened or separated by the shock wave. In order to simulate this situation, an investigation with the model modified to permit control of the flow divergence downstream of the shock wave was initiated. In an inviscid flow, the divergence of the subsonic flow would increase the adverse pressure gradient above that observed in the flat plate case. The influence on the interaction of changes in the subsonic boundary geometry that are representative of airfoils can, in principle, be investigated with the current model arrangement.

It is the purpose of this report, specifically, to document the effects on transonic shock wave-boundary layer interactions of variations in

unit Reynolds number, Mach number and subsonic boundary geometry. These effects were investigated during the last contractual period under sponsorship of AFOSR. However, the influences of the other parameters that affect the interactions will be discussed as they pertain to a complete description of the flow phenomena.

The report is arranged to: a) summarize the conclusions from the study of the different parameters for which results were released in the past; and b) present, in detail, the findings of the last year of research. Following this introduction, Section 2 reviews the fundamental aspects of the experiment and describes additions to the test apparatus that were implemented in the last year of research. Section 3 gathers the results obtained in the various phases of the investigation. Subsections 3.1 to 3.5, fulfill the objective (a), stated above. They contain salient measurements and findings relative to Re_L , unit Re and of influences that were fully reported in previous OSR annual reports. T_w/T_o effects, which were presented fully in Ref. 5, are also addressed. Subsections 3.6 to 3.8, collect the measurements obtained during the last year of research (objective b, above). Measurements of shock shape, wall pressure distribution and velocity profiles document the effects on the interaction that were observed while exploring changes of subsonic boundary geometry at $Re_L = 36 \times 10^6$. Results obtained at the lower Re_L 9×10^6 and equal shock holder geometries are taken up next. Additional data relative to one shock holder geometry, which was singled out to provide a more complete data base, conclude Section 3.

The data generated by Calspan research program are compared with other experiments in Section 4. From the comparison, emerges a comprehensive description of transonic shock wave-boundary-layer interactions and interesting trends regarding the dependence of such flows on their governing parameters. Finally, conclusions that synthesize the observations made during the research are contained in Section 5.

5. Padova, C. and Wittliff, C.E., "The Effects of Wall-to-Total Temperature Ratio on Shock Wave-Turbulent Boundary Layer Interactions at Transonic Speeds," Calspan Report No. WF-6091-A-1, October 1979.

Section 2 EXPERIMENT

2.1 Calspan Ludwig Tube

The Calspan Ludwig Tube⁶ is a large scale, upstream-diaphragm facility as shown in Figure 1. The supply tube is 18.3m long and has an inner diameter of 1.1m. At the downstream end, there is located a diaphragm station which houses a quick-release cutter bar. Different interchangeable nozzles can be joined to the diaphragm station. In the present experiments, the transonic perforated nozzle was used. This nozzle is housed within a large dump tank, 2.4m in diameter and 18.3m long. The nozzle consists of an entrance section with area contraction of 1.72:1, followed by a constant area section 0.813m in diameter and 2.44m long. The constant area part of the nozzle is perforated to a porosity of 19.1%. The perforated nozzle is contained within the evacuated dump tank, and during the experiment sonic outflow through the walls expands the nozzle flow to low supersonic Mach numbers. Selective coverage of some of the perforations permits streamwise variation of the Mach number. In the present experiment, this feature was used to reproduce an airfoil-type pressure history in the boundary layer approaching the shock. A detailed description of the nozzle design and pressure distribution is given in Ref. 3.

In the operation of the Ludwig tube, a Mylar diaphragm is inserted at the diaphragm station, the nozzle and dump tank are evacuated to a pre-determined pressure, the supply tube is pressurized, and the diaphragm is ruptured mechanically. After the transient starting process is completed, a steady flow is obtained until an expansion wave travels up the supply tube, reflects from the end wall, and returns to the nozzle. Originally, the test time of the facility was about 45 ms. Later, the facility was lengthened and all the experiments discussed here were performed with about 95 ms of useful test time available.

6. Sheeran, W.J. and Hendershot, K.C., "A New Concept of a Variable-Mach Number Perforated Wall Nozzle for providing a Supersonic External Stream in Rocket-Propulsion Testing," AIAA Paper 68-238, March 1968.

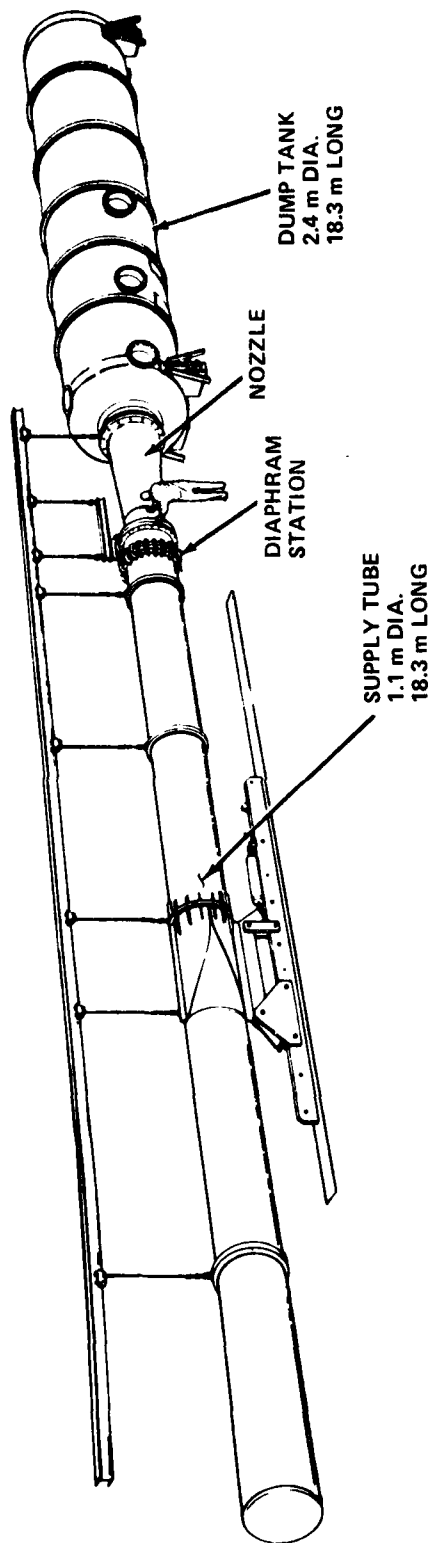


Figure 1 CALSPAN LUDWIG TUBE AND SCHEMATIC OF MODEL INSTALLATION

The early operation of the Ludwig tube was limited to experiments with the entire apparatus initially equilibrated to room temperature. At those conditions, the expansion wave propagating into the supply tube accelerated the gas and cooled it to a total temperature of about 265°K. This produced a wall-to-total temperature ratio of about 1.11 and resulted in heat transfer from the model to the gas. In order to obtain heat transfer from the gas to the model, the total temperature was increased by heating the entire supply tube with electrical heaters mounted around the exterior surface. This modification allowed the supply tube to be heated to as high as 550°K. In the present experiments, temperatures up to about 400°K were utilized. With the hot supply tube, the test gas heated up during the pressurization process and equilibrated at a uniform temperature very quickly. Five thermocouples mounted within the supply tube were used to measure the initial gas temperature and to verify its uniformity.

2.2 The Simulation Experiment

Among the basic aims of the present research was that of gathering experimental information leading to a deeper understanding of similarity requirements for scaling wind tunnel results to full-scale flight conditions. Well-known conflicting requirements for the values of the dimensionless variables that govern such scaling arise in practice when modeling of shock wave-boundary layer interactions is attempted for high-speed airfoils and aircraft configurations. Under these circumstances, partial modeling is mandatory. In conventional wind tunnel testing, in order to duplicate M and model geometry, the parameters Re_L and T_w/T_o are distorted.

In the present study, it is specifically the influence of the latter parameters on the recompression of the supercritical flow region around an airfoil that is sought. The simulation experiment is designed to provide control of Re_L , T_w/T_o and M over a range of practical values. In order to achieve this, distortion of the geometrical specification must be accepted.

The flow region that is of concern in studies of separated transonic shock-boundary layer interactions centers around the typical bifurcated shock structure. Three basic experiments may be used to simulate this flow region. First, an airfoil may be used to generate a supercritical flow and shock embedded in an essentially subsonic stream. Alternatively, a bump on a wind tunnel wall may accomplish the same objective. Finally, a shock generator (holder) may be used to develop the desired shock structure in a fully supersonic incoming stream. The experiment reported here belongs to the last category, the choice having been made on the basis of using a large scale model to permit a detailed probing of the interaction and to provide a high test Re_L . Thus, only a neighborhood of the wave/viscous interaction occurring on an airfoil is simulated.

For the experimental results to be of maximum use, conditions at the boundaries of the observed interaction neighborhood should be completely determined. In the case of the ideal flat plate that is, at least in principle, easily accomplished. The incoming flow would be described by a viscous surface boundary layer, together with the uniform parallel inviscid flow field only slightly modified by the presence of the boundary layer on the plate. The upper boundary surface, provided that it can be located far enough from the plate, consists of a streamline parallel to the plate. It is isobaric and supersonic upstream of the shock, and isobaric and subsonic downstream of the shock. Provided that the outlet surface is located far enough downstream, it also is isobaric and contains a fully developed viscous layer consistent with the local inviscid flow. The outlet flow field, however, is more complicated than the inlet flow, since the bifurcated shock introduces a slip surface. The flow length required for this slip surface to disappear completely might, depending upon the height of the bifurcation, be very long, and in a reasonable experiment it is more probable that the slip surface will be smoothed but not eliminated completely.

In none of the experiments reported here is the flow at the boundaries as simple as described above. The initial experiments performed under the present research may be viewed as an attempt to simulate, under varying

Re_L conditions, the shock wave-boundary layer interaction standing on a flat plate in an unconfined flow. A portion of the transonic test stream is intercepted with a shock holder of rectangular cross-section. This is equipped with a choking flap to form the shock and an area relief to stabilize the shock. The intercepted flow includes the test boundary layer which is approximately 35mm thick. The interaction occurs a few centimeters downstream of the shock holder entrance where the side wall and top wall viscous layers are thin. Under these conditions, the ratio of viscous to mainstream flow is small and it is determined essentially by the contribution of the floor boundary layer. While designing the experiment, the classical results of Seddon⁷ were available to estimate the viscous blockage in the shock holder channel. Those results may be interpreted to indicate insensitivity of the interaction quantities to shock holder geometry for ratios of viscous to mainstream flow up to 15%. The latter parameter is about 10% in the Calspan apparatus and the simulation experiment may be judged to represent an acceptable approximation to the unconfined shock-boundary layer interaction.

A unique feature of the present research that influenced the initial choice of the simulation scheme was the capability to impress an airfoil pressure distribution on the development of the turbulent boundary layer entering the interaction region. To this end, the experimental apparatus composed of a perforated nozzle plus shock holder was selected. Because the perforated nozzle was contained within the evacuated dump tank, there was an outflow through the porous walls during the experiment. That outflow produced a supersonic expansion which could be controlled by selectively covering the wall perforations. In this manner, a specified axial pressure distribution could be obtained in the nozzle. The technique was described in Ref. 6 and gave the axial Mach number distribution shown in Fig. 2. To the extent that the dimensions of the interaction region are small compared with those of an airfoil, the initial experiments can also be considered to represent a first approximation to a local description of the shock-wave boundary layer interaction occurring on an airfoil.

7. Seddon, J., "The Flow Produced by Interaction of a Turbulent Boundary Layer With a Normal Shock Wave of Strength Sufficient to Cause Separation," ARC R&M No. 3502, March 1960.

A continuing consideration in the Calspan research has been on the validity of the basic experiment. Early measurements were checked on how well they represented full-scale conditions by comparing them with the flight test data used to design the experiment, Fig. 2. That comparison showed that the experiments closely duplicated the flight test results ahead of, and in the immediate vicinity of the shock wave. Consequently, the high Reynolds number results should be representative of full-scale conditions. Also checked was the two-dimensionality of the experiment by measuring the spanwise distribution of static pressure about one boundary layer thickness behind the shock wave. Those results, Fig. 3, show that the pressure is uniform across the test plate within a few percent, and is not influenced appreciably by extraneous channel effects. It should be noted that all experiments can be referred to as steady and two-dimensional only in a mean sense because it is recognized that turbulence is unsteady and three-dimensional. Consequently, the interaction process is also unsteady and three-dimensional. These experiments are regarded as steady and two-dimensional in a mean sense, because the turbulent fluctuation times are small in comparison with our test time and the scale of the turbulence is small in comparison with the channel dimensions.

Recently the approach used in the experiment to model the subsonic flow region downstream of the shock was reexamined. It was recognized that direct experimental investigation of the influence of changes in the flow conditions imposed at the subsonic boundary was desirable for two reasons. First, in the Calspan experiments, as well as in most other experiments of similar type, the top boundary was too close to satisfy completely the requirements for unconfined flow. This results from a compromise between the need to obtain a high test Reynolds number and the intolerance of the transonic flow field to the blockage effect associated with the increase in boundary layer displacement thickness through the shock wave. Although the effect is believed not to be large, the top wall of the shock holder imposes a flow inclination which is not necessarily that which would exist at the same height in an unconfined flow. Second, in the interaction on an airfoil that is of

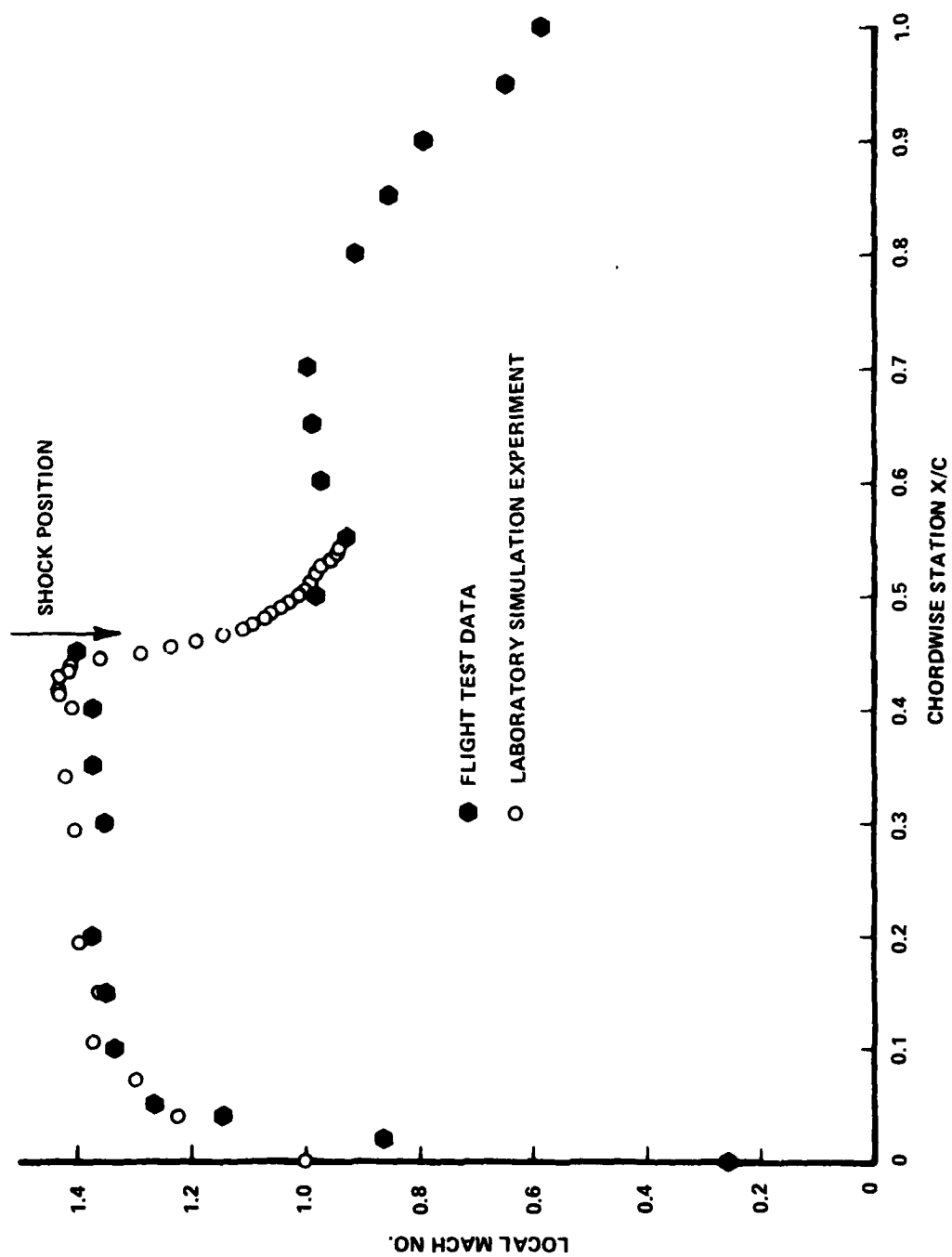


Figure 2 COMPARISON OF LOCAL MACH NUMBER DISTRIBUTION IN FLIGHT AND IN LUDWIEG TUBE

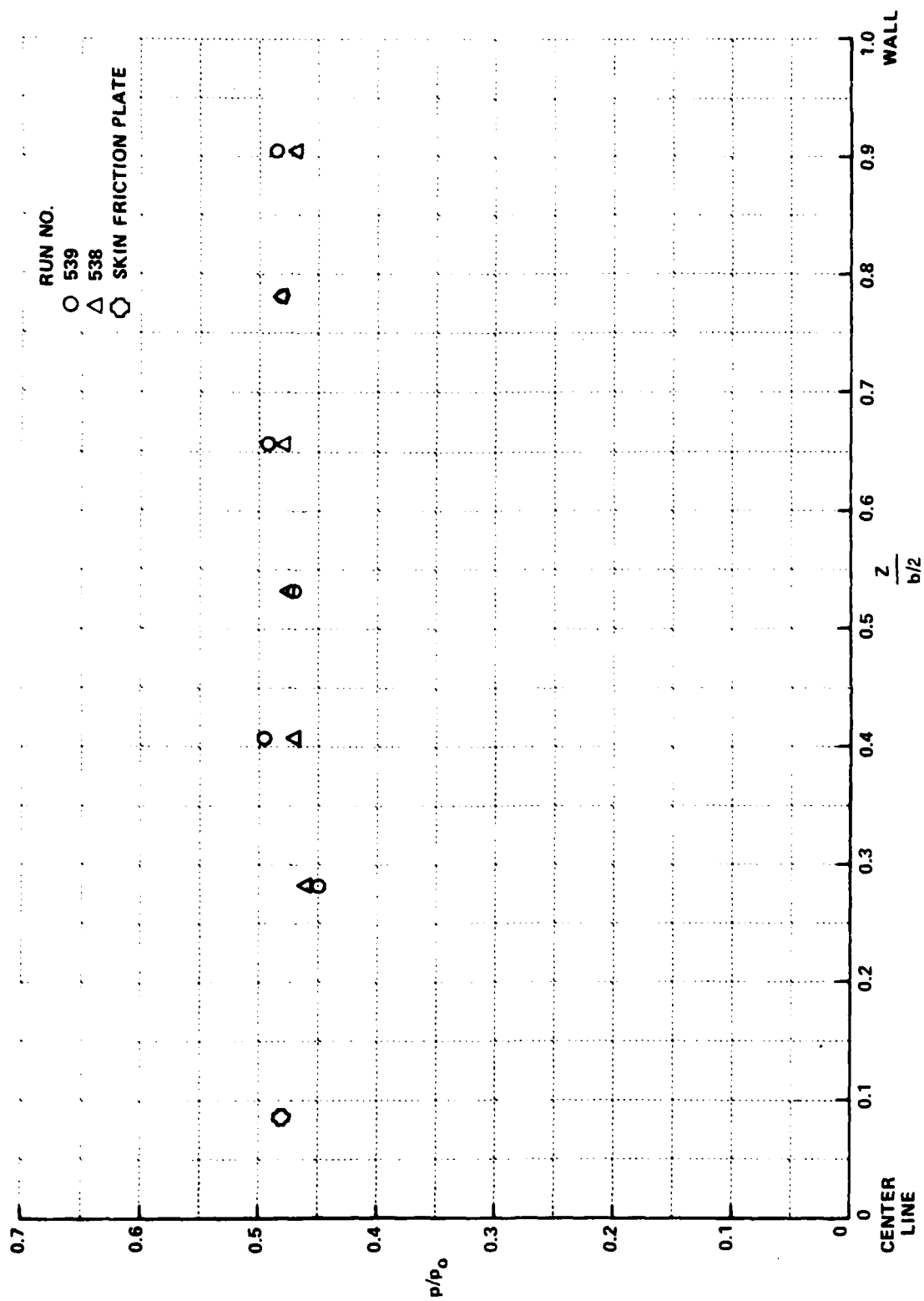
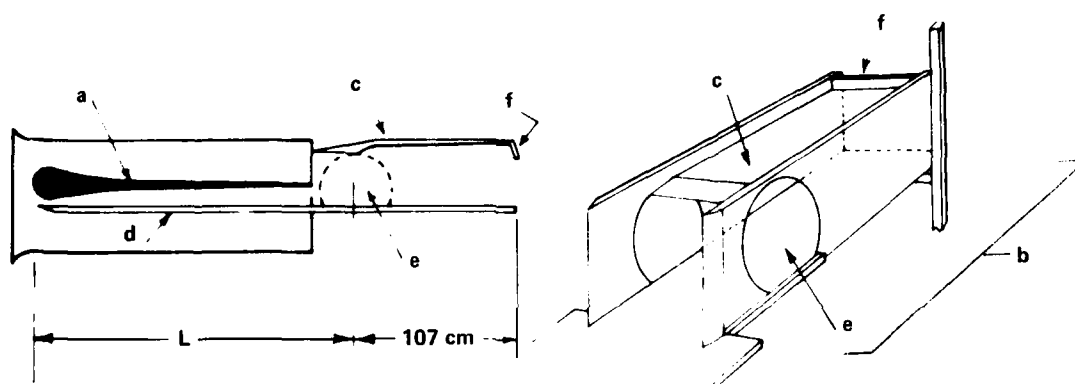


Figure 3 SPANWISE DISTRIBUTION OF STATIC PRESSURE $Re_L = 9 \times 10^6$, $x_s/\delta_u = 0.83$

practical interest, the extent of the region of strong viscous/inviscid coupling may be large enough to invalidate the flat plate approximation. A non-uniform subsonic flow is imposed by the airfoil geometry downstream of the interaction. Commonly, the shock is located in a region of adverse pressure gradient and this can be expected to delay recovery of the boundary layer weakened or separated by the shock wave.

In order to investigate the influence on the interaction of changes in the subsonic flow region, a series of experiments with the shock holder modified to include a perforated top wall was planned. This perforated model permits control of the flow divergence downstream of the shock wave. The description of the inviscid flow field may be completed by measuring the flow angle near the top plate of the shock holder or by any method yielding values for the streamline inclination. With the current model arrangement, the situation that arises on airfoils can be studied because adverse pressure gradients of controlled strength can be imposed downstream of the interaction, at least in principle. In an inviscid flow, divergence of the subsonic stream would certainly increase the adverse pressure gradient. The situation that occurs in practice, when a recovering boundary layer is present, is the subject of this study. At the same time, the experiments with the current apparatus will provide indications on the validity of the experimental model used in the past to simulate the unconfined flat plate interaction. To this end, the sensitivity of past measurements to the proximity of the holder top plate can be investigated by changing the amount and the distribution of perforation in the apparatus.

The flat plate shock holder assembly is shown schematically in Fig. 4. The flat boundary layer plate spanned the full width of the nozzle and extended either 124 cm or 241 cm upstream of the shock position. An additional 107 cm of plate downstream of the nominal shock position constituted



(a) NOZZLE WITH TAILORED POROSITY DISTRIBUTION; (b) 33 x 40 cm MODEL; (c) SHOCK HOLDER TOP PLATE; (d) FLAT PLATE (L = 124 cm OR 241 cm (e) OBSERVATION WINDOW; (f) CHOKING FLAP

Figure 4 TEST APPARATUS

the bottom wall of the shock holder flow channel. A steady boundary layer flow, as evidenced by pitot pressure, static pressure and skin friction, is established on the floor plate about 15 ms after the start of the experiment. This is consistent with the time required to establish turbulent boundary layers as measured in Ref. 8.

The shorter boundary layer plate was used for the studies of unit Reynolds number effects. The modified apparatus is shown in Fig. 5. The configuration was also used for the heated supply tube tests. With the shortened flat plate, the porosity distribution was changed, as indicated.

The flow downstream of the nozzle exit is constrained by a rectangular shock holder flow channel 40.6 cm wide with height depending, as described later, on the geometry used for the upper shock holder plate. The side walls of the rectangular channel extend a few centimeters into the nozzle exit and divert the thick nozzle boundary layer. The flow is choked with an adjustable flap at the exit of the shock holder channel. It is this flap that, during the starting process, sends a shock wave system upstream through the channel and produces the desired shock wave-boundary layer interaction.

The selection of the shock holder, which is used to stop the traveling shock wave and stabilize it at a fixed position, is an important aspect of the experimental design. A propagating shock can be weakened and positioned at a fixed location by decreasing the mass flow per unit area behind it. This can be accomplished by introducing an area change in the flow channel or by removing mass along the shock holder. The first scheme was used in most of the experiments performed during Calspan's research program. The early Re_L experiments and the unit Re_L , M number and temperature ratio investigations were all carried out in such a shock holder. It is recalled schematically in Fig. 6A. The channel entrance height is 28 cm. The area

8. Davies, W.R. and Bernstein, L., "Heat Transfer and Transition to Turbulence in the Shock-Induced Boundary Layer on a Semi-Infinite Heat Plate," J. Fluid Mech., Vol. 36, Pt. 1, pp 87-112, 1969.

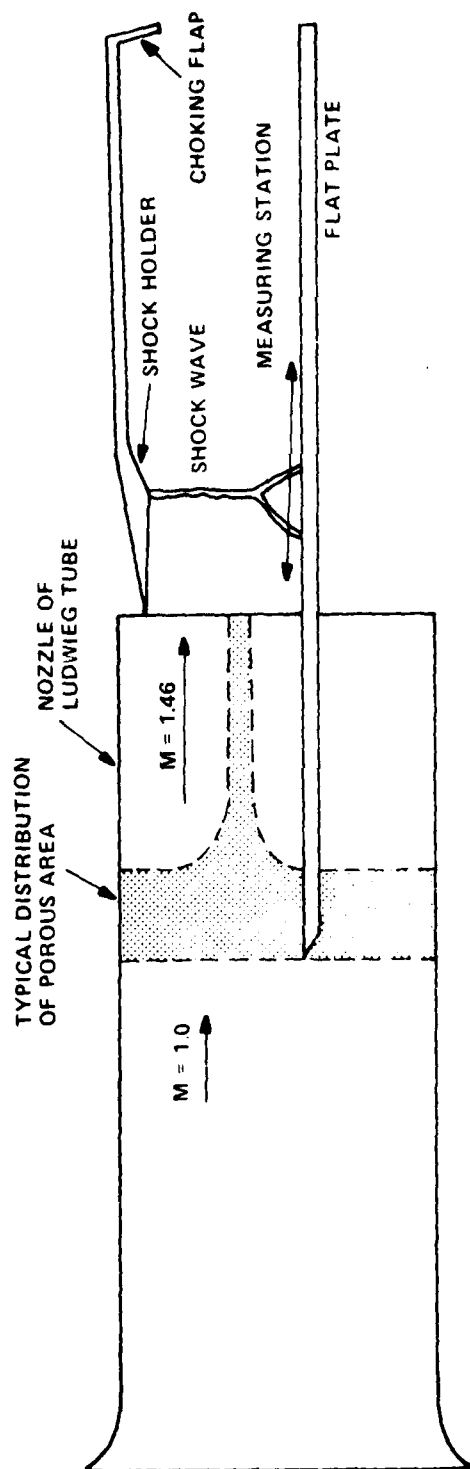
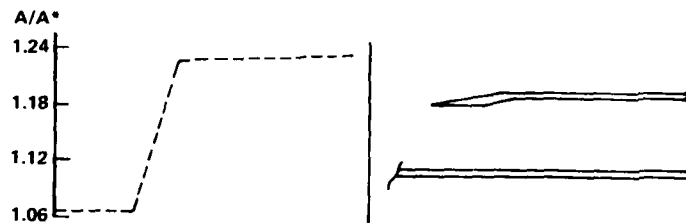


Figure 5 MODIFIED TEST APPARATUS

A. AREA RELIEF MODEL



B. PERFORATED MODEL



POROSITY DISTRIBUTIONS

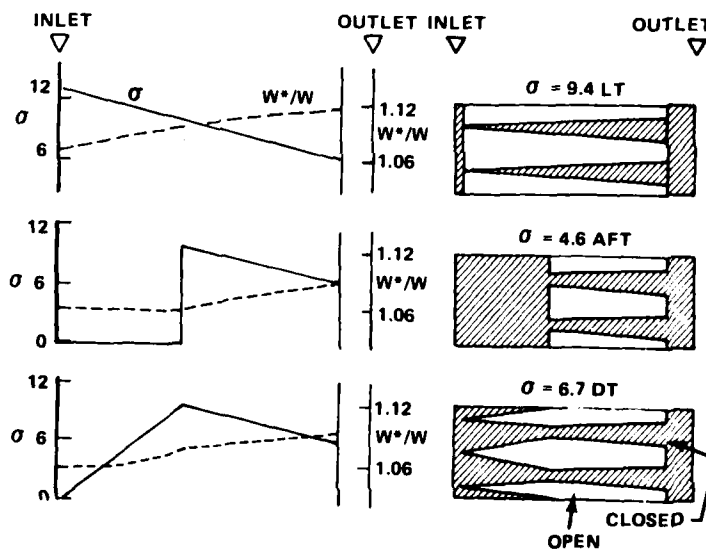


Figure 6 SHOCK HOLDER CONFIGURATIONS

change is formed by a ramp on the top wall of the shock holder, 10 cm long, which increases the flow channel height to 33 cm. During the starting process the choking flap sends a wave system upstream through the channel. The upstream progress of the wave system is halted by the area change. The normal shock wave so formed remains stable at its test position for a period of 6 to 15 ms, which is adequate to permit the flow to stabilize and the data to be taken.

The later tests used mass removal through the top wall to stabilize the shock. The ramp was removed from the top wall and replaced by perforations (12.5% open area) that extend from 2.8 cm behind the leading edge to a point near the exit of the model. Removal of the ramp increased the entrance height to 33 cm, and the resultant channel is one of constant cross-sectional area. With this shock holder, the wave system can be stabilized nearly anywhere along the length of the model, either within the model or external to its forward lip. In general, stationary shock structures lasting 15 to 25 ms are found to be possible with this model.

By blocking some of the perforations in the top plate, it was possible with this configuration to vary the boundary conditions downstream of the shock wave. Three different perforation distributions are compared with the original area relief shock holder in Fig. 6. A simple one-dimensional (1D) characterization of the flow is used to describe each shock holder. The area relief holder is described in terms of the variation along its length of the ratio of local cross-sectional area to the critical value for the flow downstream of a normal shock at the test Mach number (A/A^*). Idealized reference values for all flow quantities are then available using 1D isentropic relationships. The perforated shock holder is described in terms of the variation along its length of the ratio of the critical mass flow per unit area (for the flow downstream of a normal shock at the test Mach number) to the local mass flow per unit area (W^*/W). In calculating the latter, the outflow through the perforations was taken to be that which would occur if the choked outflow were driven by the full stagnation pressure downstream of a normal shock with an orifice coefficient equal to 1.0. In the 1D characterization, the quantity W^*/W corresponds directly to the quantity A/A^* of a constant-

mass-flow-rate channel and comparison of any flow quantity occurring in the perforated or area relief holder configuration is straightforward.

The three different porosity distributions of Fig. 6B are labeled according to their average open area as percentage of the total top wall area (σ). The streamwise distribution of σ along the top wall is also given in each case. In the first (top to bottom) configuration σ varied linearly from the leading edge of the plate, where the full 12.5% of porosity of the top plate was open, to a point near the choking flap, where half the perforations were closed off. The average porosity was therefore 9.4% and the configuration is designated 9.4 Linearly Tapered. In the second configuration, called 4.6 AFT, the open area was concentrated toward the downstream (aft) end of the plate and the average porosity was 4.6%. In the third configuration, the average porosity was 6.7% and the open area was doubly tapered. Tests were also made using other configurations, but only the above three are discussed in detail in this report.

Instrumentation

The basic instrumentation and data reduction procedure used in this apparatus are described in Ref. 3. In summary, the instrumentation includes a set of pitot-static rakes (Fig. 7) any of which may be mounted on a 12.7 cm long base plate containing the pressure transducers. The base plate may be mounted flush with the floor plate at various stations along the flow channel. In addition, a second plate shown in Fig. 8, incorporates a set of 10 pressure orifices and transducers and 10 piezoelectric skin friction transducers. This plate may also be located at various streamwise positions to generate closely spaced pressure and skin friction data points.

All of the transducers used in the basic instrumentation are piezoelectric devices developed at Calspan. They are described in Ref. 9 and 10.

9. Bogdan, L., "Instrumentation Techniques for Short-Duration Test Facilities," Calspan Report No. WTH-030, March 1967.
10. MacArthur, R.C., "Contoured Skin Friction Transducers," Calspan Report No. AN-2403-Y-1, August 1967.

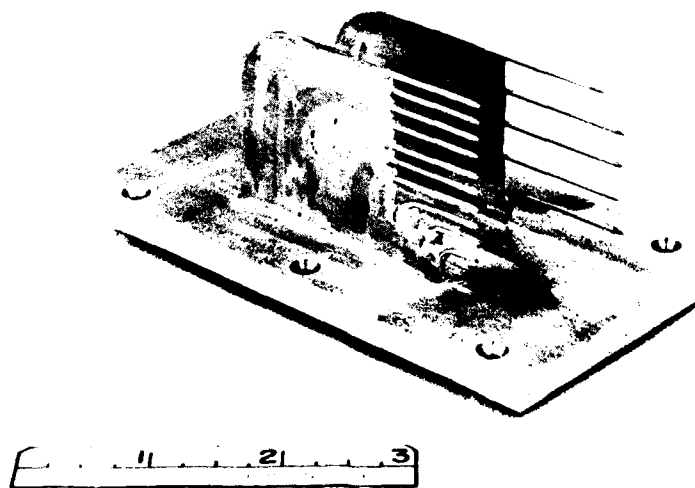
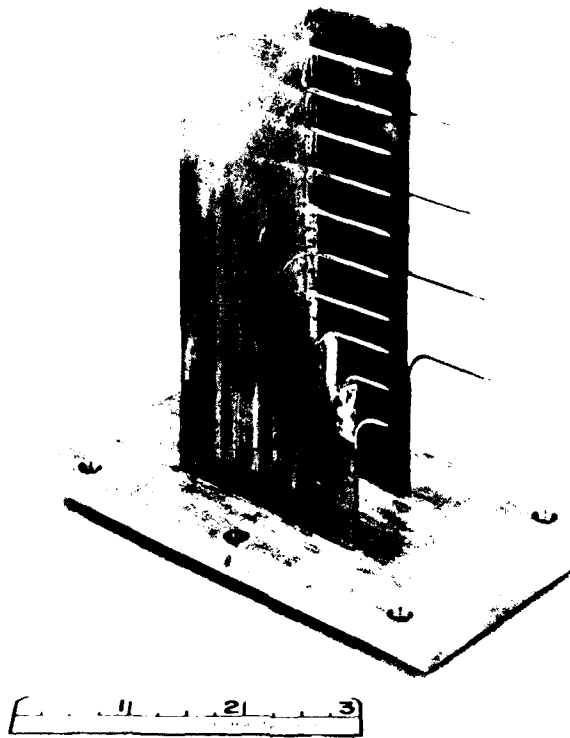


Figure 7 TYPICAL PITOT-STATIC RAKES

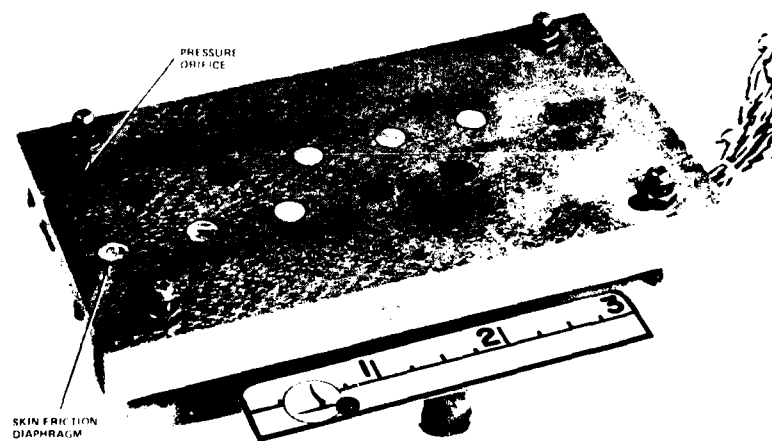
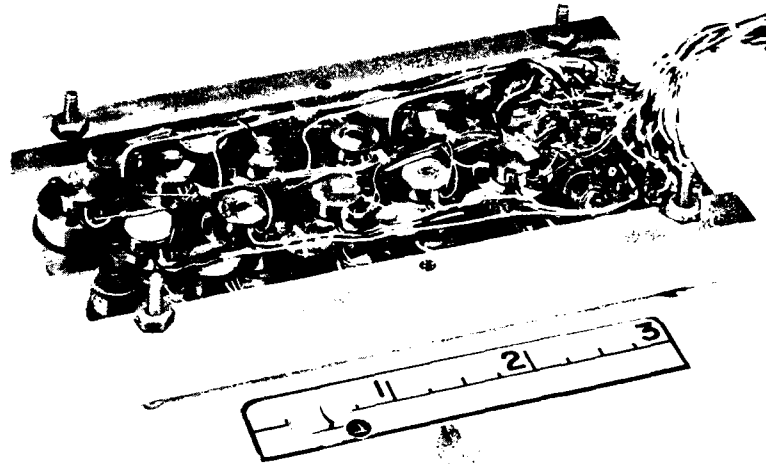


Figure 8 SKIN FRICTION - SURFACE PRESSURE SURVEY PLATE

Each transducer is compensated internally to minimize acceleration effects and typically they are linear to within $\pm 2\%$. The pressure transducers have a full-scale range of 690 kPa and a nominal sensitivity of 7.25 mv/kPa. The skin friction transducers have a 6.4 mm diameter sensing surface and can measure skin friction up to 140 Pa. Typically, they have a skin friction sensitivity of 3620 mv/kPa and a pressure sensitivity of 0.7 to 3.0 mv/kPa. The skin friction transducers were calibrated for pressure sensitivity and corrections were applied to the skin friction data. This was accomplished using the surface pressure measured adjacent to each skin friction transducer, Fig. 8.

Schlieren observations of the flow field were made using a high-speed framing camera operating at a rate of about 7000 frames per second. This diagnostic was used to determine the shock position along with other structural features of the flow.

During the past year, the principal change in the apparatus involved the new shock holder described in the preceding section. Additions to the instrumentation deployed have also been made. A pitot-static rake, tall enough to span the full height of the flow channel (Fig. 9), was fabricated. This was found to be necessary because earlier data had not, in all cases, reached a clear cut inviscid condition. It should be noted that it is necessary to survey not only through the height of the normal viscous boundary layer, which is increased by the interaction with the shock wave, but it is also necessary to carry the measurements through the height of the non-uniform region behind the lambda shock and the lower portion of the normal shock wave, where it is in fact a strong oblique wave. In experiments with an adverse pressure gradient, the height of the non-uniform region was expected to be greater.

A row of "permanently" installed pressure transducers has been installed in the floor plate, (Fig. 10) to supplement the pressure measurements obtained with the movable skin friction plate. The permanent pressure transducers permit shock trajectories to be determined in all runs and provide

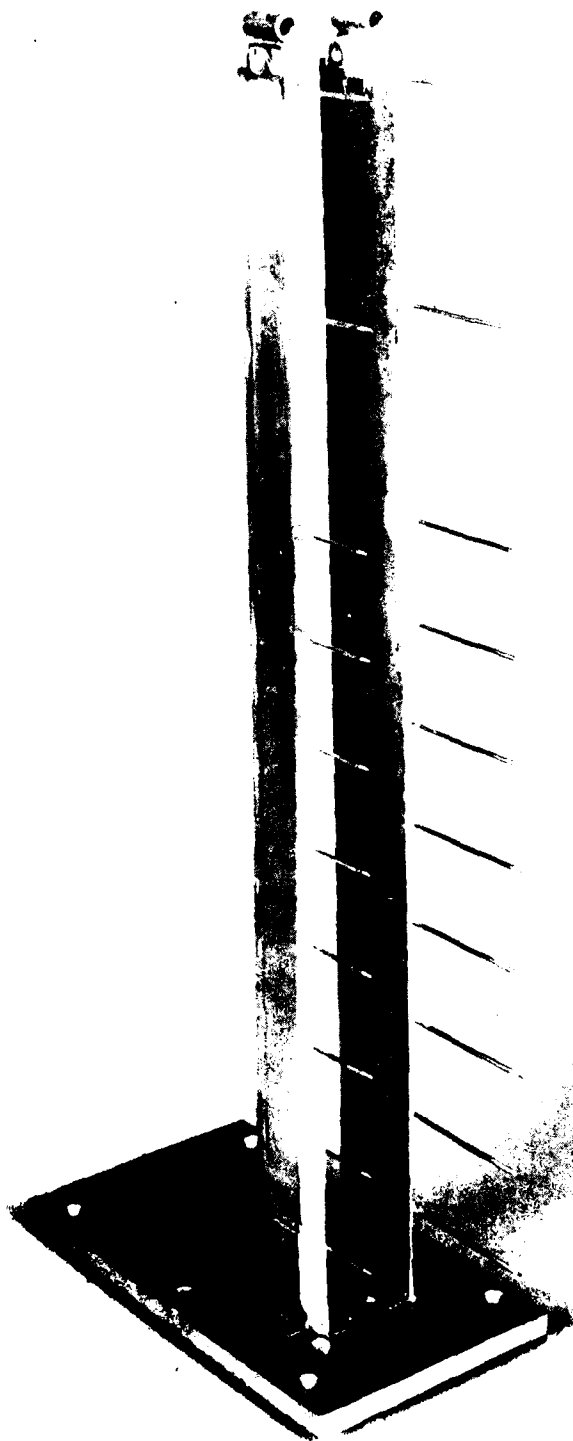
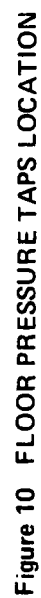


Figure 9 RAKE SPANNING FULL MODEL HEIGHT



pressure measurements over the full plate length. Provision has been made for relocating this row of transducers to locations closer to the sidewall, when desired, to assess the two-dimensionality of the shock structure.

Recently, in order to complete the data, a flow angle probe (Fig. 11) has been added to the instrumentation deployed during the tests. The probe consists of two hypodermic tubes with an o.d. of 0.813 mm and an i.d. of 0.508 mm. The two tubes are mounted side-by-side and their ends (shown enlarged in Fig. 11) are beveled to $\pm 45^\circ$ to the centerline direction. The difference in pressure between the two tubes which originates from a stream approaching with a pitch angle is measured with a Kulite Mod. XT-190-5D differential pressure transducer. This transducer has a rated pressure of 34.5 KPa and a sensitivity of 1.24 mV/KPa. The transducer is housed in a streamlined box that is mounted on the shock holder wall outside the main test flow. One of the hypodermic tubes is directly connected to the reference port of the transducer. The other tube is connected to the cylindrical case in which the transducer is threaded. The transducer diaphragm senses the pressure in the small adjustable volume that exists between the transducer and the case. Changes in this volume allow differences in pressure rise which may arise during the fill time to be balanced out.

Data recording and processing is now being aided by a new Digital Data Acquisition System¹¹. The DDAS includes a Varian minicomputer which has the potential to assume the major part of the data processing function.

2.5 Data Reduction

The test conditions in the Ludwig tube were determined by measuring the temperature and pressure in the supply tube immediately before the diaphragm was ruptured, and by measuring the total pressure ahead of the nozzle

11. Wittliff, C.E., Pflueger, P.G. and Donovan, P.J., "A High-Speed Digital Data Acquisition System for Short-Duration Test Facilities." International Congress on Instrumentation in Aerospace Simulation Facilities, Monterey, CA, 24-26 September 1979.

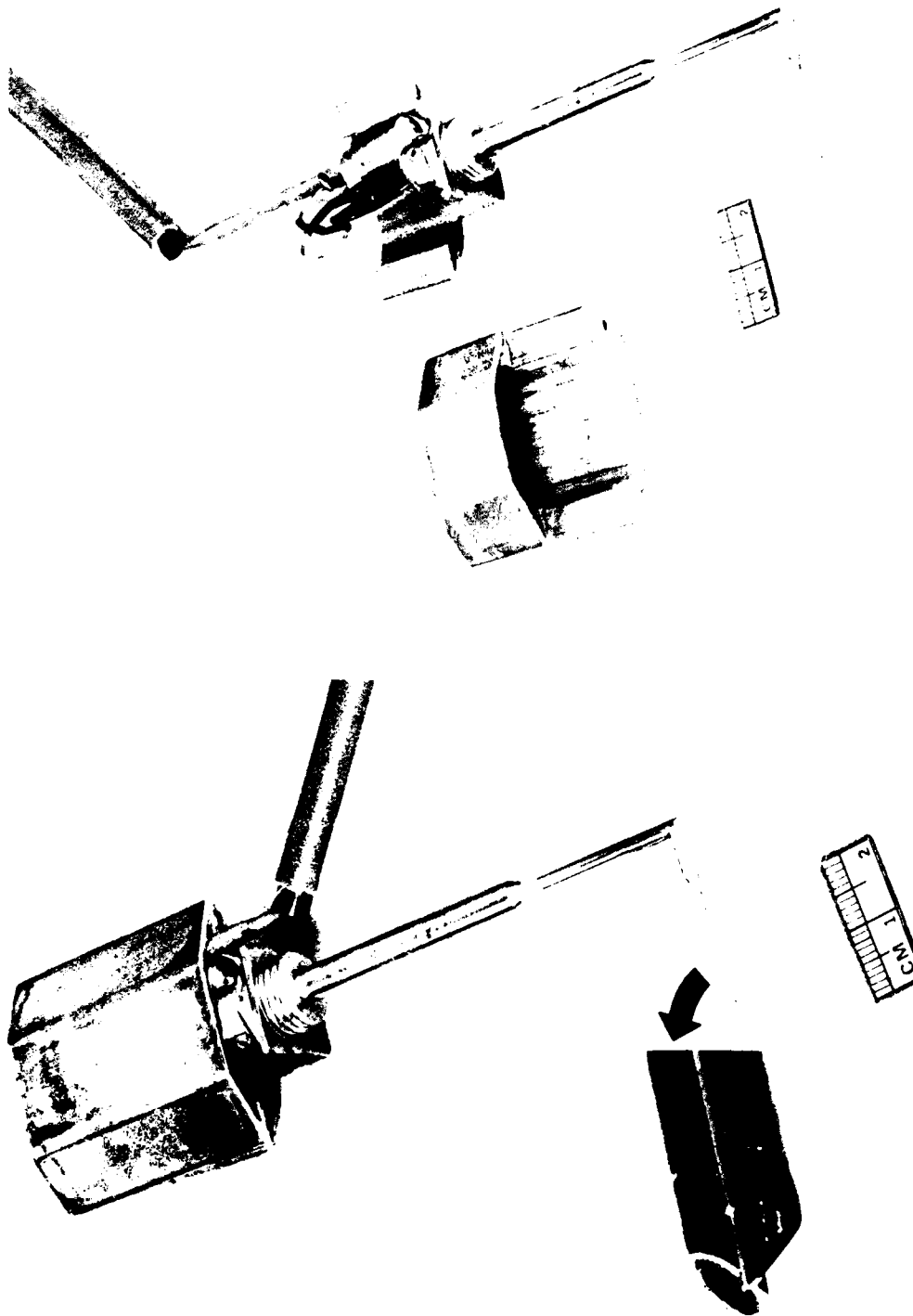


Figure 11 FLOW ANGLE PROBE AND TRANSDUCER

throat during the experiment. These were used with the isentropic relations and the relation for a centered expansion wave to determine the ambient gas properties.

The pitot pressure and static pressure data obtained in the flow field surveys were reduced to Mach number profiles using the isentropic relations and taking account of the normal shock losses in pitot pressure. It was assumed that the measured static pressure was the true local static pressure. This was verified by comparing these with the wall pressure measured without the rake present.

In compressible flow, the reduction procedure from rake pressure measurements to velocity profiles is an approximate one. This results in a dependence of the reduced velocity profile on physical assumptions made and empirical constants required (for example, recovery factor). When deriving characteristic or integral parameters from the velocity profiles, the error intrinsic to the approximation is susceptible to amplification or reduction, depending on the calculation procedure. The latter, in turn, is constrained by the amount of instrumentation deployed in the test, namely skin friction balances, temperature probes, etc. Only limited concurrence is found in the literature on the relative accuracy of commonly used data reduction procedures in relation to flow regimes and principal parameters of interest^{12,13,14}. This available basis, however, confirms the judgment that the uncertainty associated with the reduction of velocity profiles is irrelevant in relation to the quantitative understanding of the shock wave-boundary layer interaction set forth in this and previous studies.

12. Adcock, J.B., Peterson, J.B. and McRee, D.I., "Experimental Investigation of a Turbulent Boundary Layer at Mach 6, High Reynolds Number and Zero Heat Transfer," NASA TN D-2907, July 1965.
13. Winter, K.G. and Gaudet, L., "Turbulent Boundary-Layer Studies at High Reynolds Numbers at Mach Numbers Between 0.2 and 2.8," R.A.E. RM No. 3712, December 1970
14. Mabey, D.G. and Sawyer, W.G., "Experimental Studies of the Boundary Layer on a Flat Plate at Mach Numbers from 2.5 to 4.5," R.A.E. RM No. 3784, September 1974.

In the present experiments, the Mach number profiles were reduced to velocity profiles using the assumption of constant total enthalpy through the boundary layer. The validity of this assumption was checked by comparison with calculations based on the more rigorous quadratic relationship between static temperature and velocity profile in the boundary layer with heat transfer. A constant temperature recovery coefficient of 0.88 and the appropriate heat transfer parameter for the given test conditions were used in this case. The constant total enthalpy assumption proved to be adequate to compute the velocity profiles, since it results in differences of only a few percent in the region that is most affected, i.e., near the wall. However, the quadratic temperature distribution was used in computing the integral parameters of the velocity profiles.

Skin friction measurements reduction is, in principle, straightforward. To a first approximation, the transducer output is directly proportional to the shear stress on the sensing diaphragm, and only a calibration constant is required to reduce the data. The calibration constant is obtained by applying a known shear load and recording the transducer output. In practice, the skin friction transducers are affected by accelerations and pressure. All Calspan transducers are acceleration compensated and their ratio of skin friction to pressure sensitivity is better than 1000 to 1 as confirmed by calibration records. Nevertheless, due to the latter, characteristic pressure corrections are required in the data reduction when near-zero skin friction measurements are taken. In this case, the reduction procedure is further complicated by the fact that the pressure sensitivity is time dependent and varies significantly with each individual transducer. In reducing measurements from the present experiments, the pressure measured adjacent to each skin friction transducer was used to apply the required correction. In addition, an effort has been made to use the transducers with the highest friction-to-pressure sensitivity ratio to establish low scatter reference points along the measured skin friction distributions.

The flow angle probe senses pressure differences at the mouth of two tubes beveled at $\pm 45^\circ$. The output of the differential pressure transducer was reduced to flow angle values using the empirical relationship:

$$\frac{\Delta p}{q} = C_1 \alpha + C_2 \quad (1)$$

with $C_1 = 0.038$ and $C_2 = -0.094$.

Equation (1) was obtained in a continuous flow tunnel for discrete values of α between -12 and $+12$ degrees. The values of the constants C_1 and C_2 were found to be essentially independent of M in separate tests at $M = 0.6$ and 0.9 . In all of the flow angle data reduction, the above calibration relationship was used together with the dynamic pressure computed in the supersonic or subsonic flow, depending on measurement location. Normal shock equations and measured test conditions were used in computing the dynamic pressure.

All reference conditions used in presenting the data, such as Reynolds number and dynamic pressure, are computed for conditions at the leading edge of the model where the Mach number is equal to 1.0.

Section 3

RESULTS

3.1 Review of Re_L Effect in Area Relief Holder

The investigation of the influence of Reynolds number on transonic shock-wave-boundary layer interactions constituted the original purpose of the Ludwig tube simulation experiments. Results documenting that there is a strong Reynolds number influence on the shock structure and on the other quantities describing the flow field were acquired prior to the contractual period covered by this report. Many of these results have been reported in Ref. 3. However, additional analysis of the data acquired during the early experiments has followed. This analysis was performed at various times in response to questions arising within the more recent unit- Re , Mach number and subsonic boundary geometry investigations. A more detailed description of the influence of Re_L has thus been acquired and is reviewed in some detail in this section. Such a review provides valuable perspective in understanding the influence of the other parameters discussed in the remaining sections of this report.

All the early experiments to investigate the influence of Re_L were performed with the area relief shock holder and the long boundary layer plate described in Sec. 2.3. Reynolds numbers equal to 9, 18, 36 and 72 million were obtained by varying the density of the test flow. The Ludwig tube was operated with supply charge at ambient temperature. As a result, all data points were taken with some heat transfer taking place from the model to the flow ($T_w/T_o = 1.11$). The nozzle porosity was tailored for a constant Mach number of subscripts 1.43 in the neighborhood of the desired shock location.

The shock-free flow field was probed in detail for the two Re_L values 9 and 36 million. For these test conditions, pitot and static rake measurements of the undisturbed boundary layer gave directly its thickness and velocity profile characteristics. These measurements confirmed also an incoming flow essentially at the nominal Mach number in spite of noticeable perturbations indicated by the surface measurements of pressure and skin

friction. Detailed measurements are reported in Ref. 3. Briefly, the incoming flow conditions defining the interaction can be stated as in Table 1.

Table I. UNDISTURBED BOUNDARY LAYER PARAMETERS.

Re_L	M	T_w/T_o	δ (mm)	δ^* (mm)	θ (mm)	H	n	$C_f \times 10^3$
9×10^6	1.43	1.11	34.64	6.88	2.79	2.46	7.80	2.1
36×10^6	1.43	1.11	33.88	5.97	2.59	2.304	8.46	1.8

As expected, changing the Re_L altered the initial boundary layer. The fourfold increase in Re_L of Table 1 resulted in thinning of the viscous layer by a few percent, a fuller velocity profile (7% decrease in form factor) and reduced skin friction. Computational checks on the measured undisturbed turbulent boundary layer were reported in Ref. 3. Here it is emphasized that the experiments well represent, in the upstream definition of the interaction, an airfoil of fixed geometry flown at transonic speeds and varying Reynolds number. The Re_L values spanned were typical of conditions from wind tunnel to full flight. The boundary layer at the shock location was approximately constant in thickness, but its velocity profile characteristics changed depending on Re_L .

The interaction flow field was found to be remarkably affected by changes in Reynolds number. The fourfold reduction in Re_L from 36×10^6 to 9×10^6 brought about a nearly twofold decrease in the extent of the interaction, both crosswise and streamwise. Such decrease is indicated by schlieren records of shock bifurcation height and by features of the wall pressure distributions. The reduction in the length of separated flow, as evidenced by direct skin friction measurements, is even larger.

The salient aspects of the observed Re_L influence on the shock structure are recalled in the sketch of Fig. 12, based on schlieren records. It is emphasized that the actual interaction is steady only in a mean sense

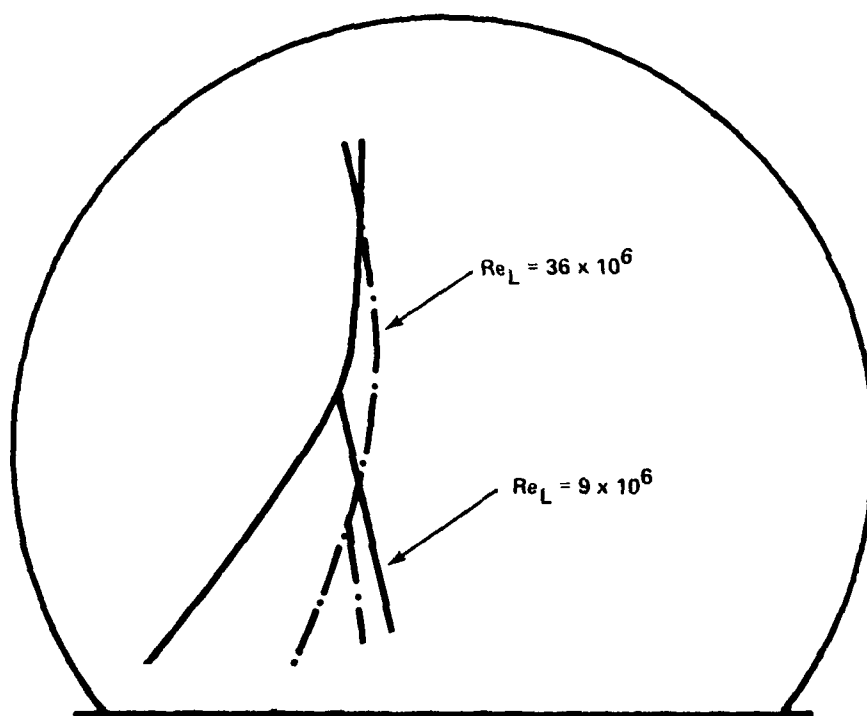


Figure 12 EFFECT OF Re_L ON SHOCK STRUCTURE

and that fluctuations in the structure of the shock are noticeable from frame to frame in schlieren movies. However, these fluctuations do not invalidate the comparison of Fig. 12 as representative of averaged main features. The upper shock occurs in the mainstream at a nearly constant location, but differences in its curvature result in a bifurcation point somewhat downstream at the highest Re_L . Accurate readings of the angles formed by the upper, forward and rear shock legs with the incoming flow are not possible from schlieren records. On the other hand, a trend for these angles to increase with increasing Re_L is apparent. Steepening is more pronounced for the upper shock branch than for the branches in the bifurcated foot. In turn, the forward shock leg steepens more than the rear one. In summary, the main observation regarding the influence of Re_L on shock structure is that the upstream propagation through the boundary layer of the first disturbance induced by the shock is lessened. To this corresponds the reduction in shock bifurcation height which has already been pointed out. The proportionality between the two is somewhat moderated by an increase in forward shock angle as Re_L increases.

Wall pressure distributions at $Re_L = 9, 18, 36$ and 72 million were reported in the past^{3, 15}. Table II summarizes the observed Re_L influence on parameters that describe the essential features of the generalized pressure rise occurring in transonic shock-wave interactions. With reference to the sketch of Fig. 13, the tabulated parameters are defined as: beginning of sharp linear pressure rise (x_u), end of sharp pressure rise (or kink pressure location, x_k), kink pressure level ($[P/p_o]_k$), slope of sharp pressure rise ($\frac{\Delta(P/p_o)}{\Delta x}$), and recovery relative to normal shock reference level at fixed streamwise location (η).

15. Wittliff, C.E. and Vidal, R.J., "Transonic Separation," ONR Project No. NR 061-18519-4-70 (438) Annual Progress Rept., December 1973.

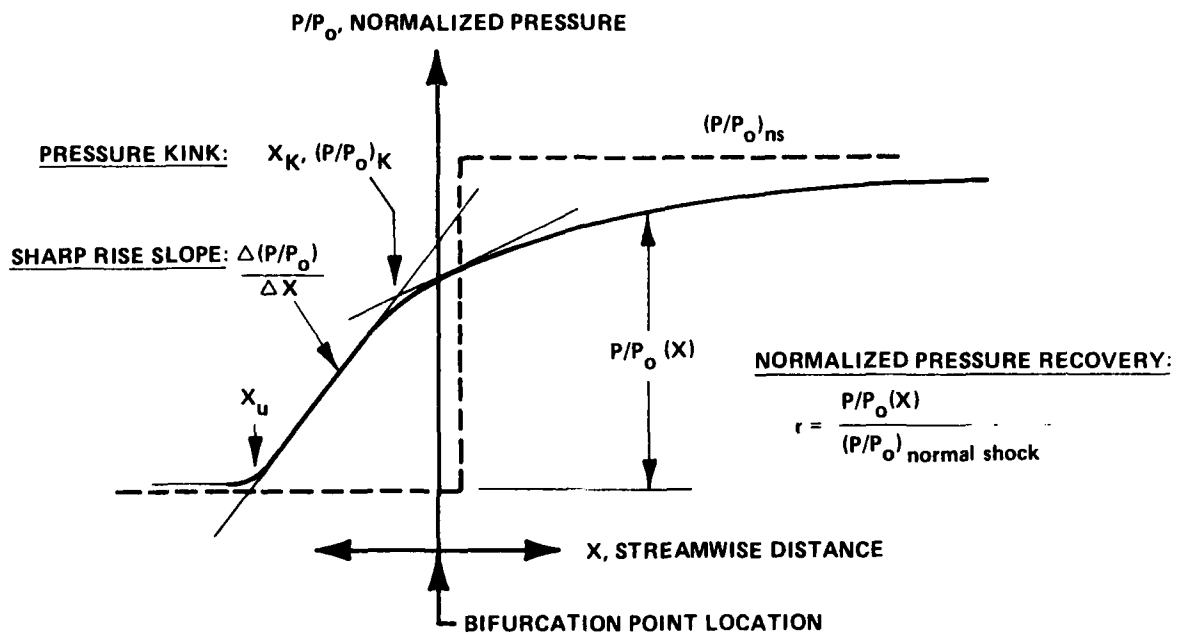


Figure 13 GENERALIZED WALL PRESSURE

Table II. Re_L EFFECT ON WALL PRESSURE PARAMETERS PRE-SHOCK $M = 1.43$,
NORMAL SHOCK RECOVERY $(P/P_0)_{ns} = 0.668$.

Re_L	δ (mm)	x_u/δ_u	$\frac{ x_k - x_u }{\delta_u}$	$\frac{\Delta(P/P_0)}{\Delta x}$	$(P/P_0)_k$	$\frac{x}{\delta_u} = 5$	$\frac{x}{\delta_u} = 10$
9×10^6	34.64	4.8	4.2	0.027	0.45	73%	84%
18×10^6	34.26*	3.4	3.9	0.033	0.48	79%	-
36×10^6	33.88	1.6	2.3	0.060	0.48	82%	85%
72×10^6	33.5	0.7	2.3	0.080	0.53	85%	-

* estimated values.

The upstream propagation of the initial sharp rise in pressure is indicated in Table II by the normalized distance x_u/δ_u . Upstream propagation was found to decrease consistently as the Re_L increased. This correlates directly with the results from visual observation of the shock structure. The initial sharp rise in pressure is known to display a fairly linear dependence on streamwise distance. The slope of this wall pressure region was found to have a nearly threefold increase as Re_L increased from 9 to 72 million. A break point (kink pressure point as termed in airfoil work by Pearcey and others) can be discerned in the surface pressure distribution. Downstream of it, the pressure rises at a reduced rate with accentuated non-linear character. The kink pressure level was found to increase with increasing Re_L . Scatter in the collected data points and the somewhat qualitative definition of $(P/P_0)_k$ can account for the anomaly in Table II at Re_L 18 and 36 million. Overall, the 18% increase in $(P/P_0)_k$ in the range 9 to 72 million of Re_L is judged representative of the true Re_L influence. Such influence dies out downstream in the moderate pressure rise as indicated by the values of τ in the table.

Seddon's⁷ classical description of transonic shock wave-boundary layer interactions distinguishes three regimes within the viscous layer. The shock phase, the displacement phase and the rehabilitation phase occur in sequence as the incoming boundary layer interacts with the shock system, and progresses to a new equilibrium with the subsonic mainstream far behind the

interaction. The distance ($|x_K - x_u|$) can be taken as an indicator of the extent of the shock phase. In Table II, the normalized value of such distance indicates that the shock phase region shrinks as Re_L increases. Concurrently, the region moves downstream from a location entirely ahead of the bifurcation point to one occurring mostly behind the bifurcation point.

Kooi¹⁶, for an interaction occurring at $Re_L = 20 \times 10^6$, $M = 1.4$, has mapped pressure distributions moving away from the wall at various distances downstream the shock system. He found that the difference between the surface pressure and the pressure in the inviscid stream decayed from an amount 25% of normal shock p/p_o level, which occurs just downstream bifurcation ($x/\delta_u \approx 0$), to 10% at $x/\delta_u \sim 5$ and to less than 5% at x/δ_u greater than 10. Negligible transverse pressure gradients characterize the rehabilitation region of the boundary layer downstream of the shock system. The values of the recovery parameter at $x/\delta_u = 10$ in Table II, indicate that this region is insensitive to Re_L changes. In contrast, the τ values at $x/\delta_u = 5$ in Table II show a 7% increase in recovery as Re_L increases. Based on Kooi's observations, this latter location falls within the displacement phase of the interaction. The results of Table II then may be interpreted to indicate decreasing Re_L influence on the wall pressure as the viscous layer progresses from shock phase to rehabilitation phase.

The interaction flow fields at $Re_L = 9$ and 36 million were probed in greater detail by measuring skin friction distributions and velocity profiles at a number of streamwise stations. Direct measurements of skin friction represent an important contribution in the investigation of shock-boundary layer interactions. In the past, much less information had been collected on skin friction than on pressure. More sophisticated instrumentation is required to measure skin friction and this results in additional difficulties in the measurement process for the same level of accuracy. However, the relevance of surface measurements other than pressure is substantial in more than one respect. The length of the region of separated flow is an important characteristic length scale of the shock-boundary layer interaction. It is a

16 Kooi, J.W., "Experiment on Transonic Shock-Wave Boundary Layer Interaction," AGARD CP-168 (also, NLR MP 75002 U), 1975.

primary indicator of the recovery of the flow downstream of the interaction. It is also likely to be one of the variables most sensitive to variations in governing parameters such as M and Re_L .

In Calspan's experiments, skin friction was measured directly with miniaturized balances. This technique has distinctive advantages over others in terms of probe interference and response characteristics. Skin friction distributions along the streamwise extent of interactions at $Re_L = 9$ and 36 million were reported in Ref. 2. Within some scatter of the data, the separation point, reattachment point and rehabilitation of the boundary layer to its equilibrium growth were directly documented.

Two kinds of observations emerged from the analysis of skin friction measurements. The first kind concerns controversial features of the surface shear distribution typical of transonic shock-wave interactions. In summary, good correlation was found between the location of the kink pressure (as defined previously) and the location of the separation point, defined by the criterion of zero shear. The relationship between kink pressure location and separation location is relevant in modeling the interaction. The two locations were found to coincide in some of the available measurements^{7,16,17}, but not in others^{5,18}. In addition, the negative C_f in the region of separated flow were found to be only a small fraction of the undisturbed skin friction level. The absolute minimum in the distributions occurred somewhat behind the bifurcation point. These results contrast in some respects with later Calspan measurements. No similar data from other experiments is available, to the best of our knowledge. The discrepancies remain unexplained.

17. Little, B.H., "Effects of Initial Turbulent Boundary Layer on Shock-Induced Separation in Transonic Flow," von Karman Institute for Fl. Dyn., Tech. Note 39, October 1967.

18. Mateer, G.G., Brosh, A. and Viegas, J.R., "A Normal Shock-Wave Turbulent Boundary-Layer Interaction at Transonic Speeds," AIAA Paper No. 76-161 presented at the AIAA 14th Aerospace Sciences Meeting held in Washington, D. C., January 26-28, 1976.

The second kind of observation concerns the Reynolds number influence on the skin friction measurements. The surface shear distributions are characterized by a sharp drop to a negative minimum from the undisturbed positive value at the beginning of the interaction. The sharp drop occurred approximately two undisturbed boundary layer thicknesses upstream of the bifurcation point at the lower Re_L , 9×10^6 , and 0.75 such units upstream at the higher Re_L , 36×10^6 . This concurs with the downstream movement of the viscous shock phase inferred from wall pressure. The skin friction drop continues beyond the zero value, defining the beginning of the region of separated flow. Following a minimum at negative C_f , the wall shear distribution recovers positive values, defining reattachment. The length of the separated flow region was found to be very sensitive to variations in Re_L . It decreased from approximately 8.5 to 2 times the undisturbed boundary layer thickness for the fourfold increase in Re_L . Concurrently, the onset of separation moved only slightly downstream. It is thus the reattachment point that is strongly influenced by Re_L variations.

Velocity profiles, obtained in the interaction flowfield at $Re_L = 9$, and 36×10^6 and 72×10^6 , were reported originally in Refs. 3, 19 and revised in Ref. 15. In summary, the velocity field characteristics were found in good agreement with the skin friction measurements in regard to the development of the boundary layer during its displacement phase. Furthermore, an interesting feature of the streamwise velocity component at some distance from the wall was displayed. The profiles just downstream of the shock system exhibited an overshoot in that the local velocity in a region within the shear layer exceeded the velocity at its edge. At $2 \delta_u$ downstream of the normal shock, Mach number profiles (reported in Ref. 19) showed a maximum of 0.9 essentially unchanging over the range of Re_L tested. The distance from the wall where the maximum occurs was measured to have decreased from $y/\delta_u = 2.5$ to 1.7 and 1.3, respectively for $Re_L = 9$, 36 and 72×10^6 .

-
19. Vidal, R.J., "Wall Interference Effects in Transonic Flow," OSR Contract No. F44620-71-C-0046, Annual Inventory of Research, September 1972.

It was noted that this overshoot behavior is somewhat analogous to the supersonic tongue observed by Seddon; however, the flow in Calspan measurements remained entirely subsonic. This is markedly different from Seddon's results, in that he found a supersonic tongue extending about $8 \delta_u$ downstream from the normal shock wave. Differences in test conditions were indicated as a probable cause of the above; higher M , 1.47 and lower Re_L , 3×10^6 , define the interactions studied by Seddon. Recently, Kooi²⁰ and East²¹ have reported detailed measurements of the overshoot velocity region under increasing M . Although minor differences of results still remain, their data indicate firmly that transition from subsonic to supersonic overspeed occurs at about $M = 1.4$ and that the supersonic tongue region increases in extent with increasing M .

3.2 Summary of Mach No. Effects

Most of the experimental results collected in Calspan research have been obtained for flow conditions typical of those on the wing of an airplane, namely an airfoil-type pressure distribution on the flat plate with a Mach number of approximately 1.4 ahead of the shock wave. These conditions were chosen because they were typical for an aircraft cruising at a Mach number of about 0.8. The investigation of shock wave-boundary layer interactions at M greater than 1.4 was also deemed of interest. Interactions at higher M have practical significance, for example in maneuvering aircraft. A verification of the expected sensitivity to M of the flow under study was also desired.

A series of exploratory experiments were performed at Re_L equal to 18×10^6 and 36×10^6 . Considerable difficulty was experienced in obtaining a stable shock at the observation position. At $Re_L = 9 \times 10^6$, the shock wave could not be stabilized in the holder. The shock wave propagated forward

20. Kooi, J.W., "Influence of Free-Stream Mach Number on Transonic Shock-Wave Boundary-Layer Interaction," NLR MP 78013 U, 23 May 1976.

21. East, L.R., "The Application of a Laser Anemometer to the Investigation of Shock-Wave Boundary-Layer Interactions," AGARD CP-193, May 1976.

from the choke flap and stabilized several inches behind the holder.

The results from the test conditions at which data were measured and an explanation of the difficulties encountered in the operation of the apparatus are reported in Ref. 22. Briefly, interactions at $M = 1.62$ and $M = 1.60$ were obtained at $Re_L = 18$ and 36 million, respectively. The bifurcation height was found appreciably greater in comparison with $M = 1.4$ cases. Comparing the surface pressure data, differences between the Reynolds numbers were again found. The initial disturbances begin further upstream at 18×10^6 , and the pressures appear to be approaching a plateau lower than that at 36×10^6 . The skin friction data, confirmed the upstream behavior and showed that one effect of increased Reynolds number is a decrease in the strength of the back flow in the separated region, as indicated by the smaller negative skin friction. Based on the skin friction measurement collected, it was concluded that under some of the test conditions, the separated region acted as an area change and tended to stabilize the shock wave behind the shock holder.

3.3 Summary of Unit Re Investigation

The unit-Re investigation addressed the question of whether Reynolds number similarity is violated in transonic shock-induced separation. In the original apparatus used for the Re_L effects investigation, the Re_L had been varied from wind tunnel to full scale values by increasing the density of the test flow and keeping fixed model dimensions. The measurements obtained indicated Re_L effects are especially significant with regard to the length of separated flow downstream of the shock. The question of possible influence of unit Re changes on the separation characteristics arose naturally.

Influence of unit Re on viscous phenomena has been an open question for a decade. Furthermore, theoretical studies²³ concurrent with the

22. Vidal, R.J., "Transonic Shock-Wave-Boundary Layer Interactions," Calspan Report No. AB-5866-A-2, August 1978.

23. Vaglio-Laurin, R., "Studies of Separated Flows." Final Scientific Report Grant No. AFOSR-72-2316, New York University Division of Applied Science, Unpublished. September 1974.

experiments at the time, indicated a possible unit Re_L influence on the transformation of the inner boundary layer region for a velocity profile near separation. To investigate the length of the separation region for a higher unit Re_L , a set of two experiments were proposed. The first experiment involved the boundary layer on a 2.4 m long plate at 138 KPa supply tube pressure and the second on a 1.24 m plate at 276 KPa pressure. The Reynolds number based upon flow length from the leading edge to the shock location was the same in each experiment, 36×10^6 . When the pressure distributions measured in the vicinity of the shock wave were compared, a difference in rate of pressure rise with distance was found²² which exceeded the experimental uncertainty. On the basis of a further inspection of the existing data, the origin of the experimental discrepancy between the two sets of data reported in Ref. 22 was found²⁴ not to lie in the shock wave-boundary layer interaction. Rather, a similar failure to scale with length Reynolds number was found in the thickness of the boundary layer upstream of the shock. The failure to scale the pressure gradient through the interaction region then follows as a consequence of the discrepancy in boundary layer thickness. It appears further that the failure to scale the boundary layer thickness results primarily from the effects of surface roughness.

3.4 Summary of T_w/T_o Effects

Interest in the effect of heat transfer on the interaction arose originally from the fact that the basic Re_L investigation had been performed with a small heat transfer from the model to the flow. This resulted from operation of the Ludwieg tube initially equilibrated to room temperature as described in Sec. 2.1. The ratio of model wall temperature to total temperature of the test flow is, for the present transonic test conditions, approximately 1.11.

24. Falk, T.J. and Padova, C., "Transonic Shock Wave-Boundary Layer Interactions," Calspan Report No. AB-5866-A-3, March 1979.

Heating the Ludwig tube air supply, while keeping the model at room temperature, produced interactions at $T_w/T_o = 0.85, 1.0, 1.11$. The 1.2 m long boundary layer plate and the area relief shock holder were used. Nominal test conditions were $Re_L = 36 \times 10^6$ and $M = 1.43$ or 1.46 . Under these conditions $T_w/T_o = 0.97$ corresponds to adiabatic flow. Thus, the extreme temperature ratios tested represent symmetrical cases of heat transfer from the flow to the wall and vice versa.

The results of the investigation into the influence of heat transfer have shown that there is a strong effect on the length of the separated region, which decreases by a factor of nearly five as the temperature ratio T_w/T_o varies from 1.11 to 0.85. The onset of separation is for practical purposes unaffected by heat transfer, the net effect promoting reattachment and boundary layer recovery. Other characteristics of the interaction, such as the height of the bifurcation of the lambda shock and the surface pressure distribution, are insensitive to heat transfer effects. The findings of the T_w/T_o investigation are presented in detail in Refs. 4 and 5.

In Ref. 5, the rapid decrease in separated flow length as the free stream total temperature is decreased relative to the wall temperature is discussed briefly, as to its possible mechanisms. However, the observed interaction behavior remains unexplained. The observed temperature effect is very interesting from a research viewpoint, but it could also have important practical implications; namely, it could be a mechanism for controlling separation on existing aircraft. In addition, this behavior is potentially very significant with respect to the effect of the temperature non-equilibration on data measured in cryogenic tunnels such as the NTF. According to these results, a 10 percent error in surface temperature simulation would have the same effect on separated length as a factor of three change in Reynolds number.

3.5 Effect of Variations in Subsonic Boundary Geometry.

All of the experiments reviewed in the preceding sections may be viewed as an attempt to simulate the shock wave-boundary layer interaction standing on a flat plate in an unconfined flow. To the extent that the dimensions of the interaction region are small compared with those of an airfoil, the experiments represents a first approximation to a local description of the interaction occurring on an airfoil. However, this approximation may not always be a good one. In the airfoil case, the shock is located in a region of adverse pressure gradient, which can be expected to delay recovery of the boundary layer weakened or separated by the shock wave. The conditions at the flow boundary that define the interaction neighborhood to be modeled are not simple as in the case of the ideal flat plate. Streamline curvature imposed by the airfoil may alter the interaction by affecting the flow angles in the bifurcation region and by altering the adverse pressure gradient further downstream of the shock system. It was recognized that some degree of control of the streamline shape in the subsonic flow behind the shock system could be introduced by using a porous holder as described in Section 2.3. A set of experiments using such a porous shock holder was planned to explore the effects of variations in the subsonic boundary geometry downstream of the interaction.

The boundary layer developed on the 2.4 m long plate. The constant temperature ratio of 1.11 corresponded to Ludwig tube operation at room temperature. Operation at charge pressures of 35 and 138 kPa resulted in the test Re'_L 's of 9×10^6 and 36×10^6 , respectively.

Conditions defining the interactions

For the subsonic boundary geometry investigation, two sets of flow conditions define the interaction. First, a description of the turbulent boundary layer entering the interaction is necessary as in the past. Second, pressure and velocity must be estimated or directly measured at a suitable control surface in the subsonic region of the interaction.

The parameters defining the flow at the inlet of the interaction are independent of the porosity of the shock holder for interactions occurring near the lip. The supersonic character of the test stream assures that any model geometry feature will influence only a downstream flow region. Incoming flow quantities were measured in shock-free tests and are presented in Fig. 14 and 15.

Figure 14 shows wall pressure measurements taken on the boundary layer plate as far forward as the leading edge of the sidewalls of the shock holder ($X = -40.6$ cm). These measurements extend downstream inside the porous holder over approximately 60% of its length. Upstream of the holder lip, the Mach number attributable to the test flow, using the isentropic one-dimensional equation, shows deviations from the nominal value that are somewhat higher than expected. Inside the holder, the Mach number increases monotonically as the stream expands due to mass removal at the porous top wall.

This streamwise M distribution was found to be repeatable. The disturbances occurring upstream of the holder lip are found to have negligible effect on the incoming boundary layer, based on the skin friction measurements (Fig. 14) and rake surveys (Fig. 15). The interactions occurring in front of the holder lip are thus defined by the parameters listed in Table III. The average M corresponds essentially to the nominal value, and the integral boundary layer parameters are those of the velocity profile taken at the location $X = -76$ mm.

Table III. UNDISTURBED BOUNDARY LAYER PARAMETERS.

Re_L	M	T_w/T_o	δ (mm)	δ^* (mm)	θ (mm)	H	n	C_f
36×10^6	1.43	1.11	33.88	5.96	2.59	2.304	8.46	2.25×10^{-3}

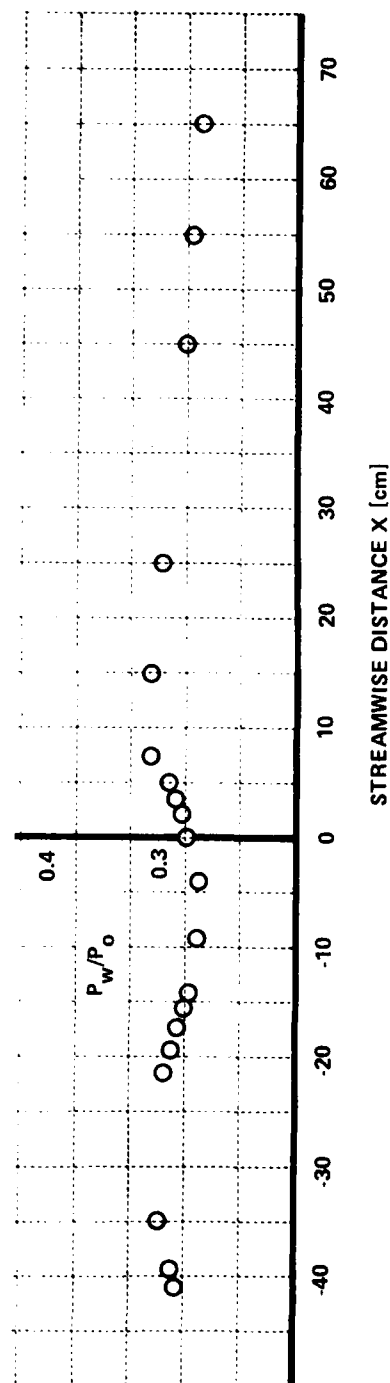
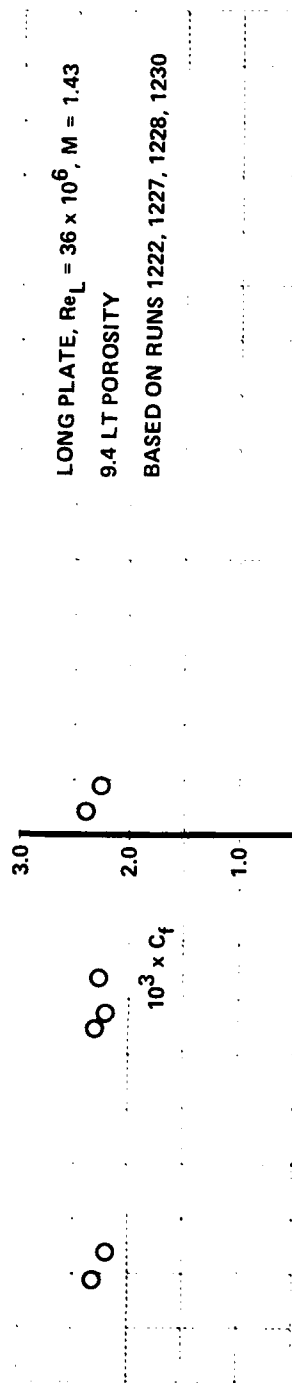


Figure 14 SHOCK FREE WALL PRESSURE AND SKIN FRICTION

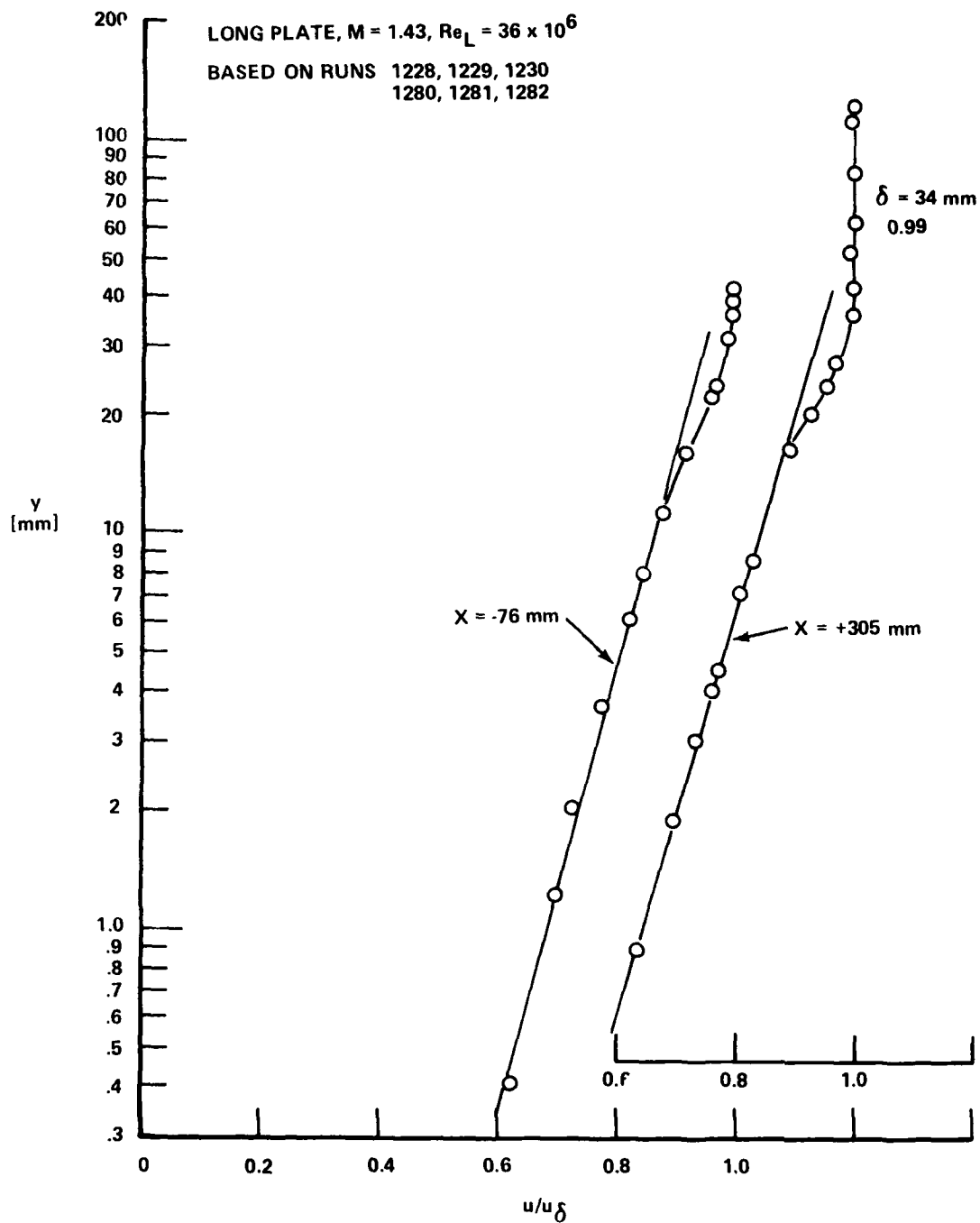


Figure 15 UNDISTURBED VELOCITY PROFILES

Interactions occurring inside the holder are also discussed briefly in the following. Based on Fig. 14, they are found to occur at slightly lower M (as low as $M = 1.38$). The velocity profile measured at the location $X = +305$ mm (Fig. 15) indicates only negligible variation in the boundary layer entering these interactions.

The second set of conditions required to define the interaction must describe the subsonic flow at a suitable perimeter downstream of the shock system. The geometry of the porous wall of the holder and its exit area are known in the present tests. Sonic flow through each of these openings can be postulated based on the static pressure known to exist inside the holder and the low vacuum tank pressure against which the flow is discharged. With some simplifying assumptions, the boundary conditions of the subsonic flow at the top wall and at the exit of the holder can be estimated. In addition, direct measurement of flow angle near the top plate was provided in some of the experiments as described in Section 2.3.

Seven porosity distributions covering values 12.5, 9.4, 6.7, 4.6, 2.2, and 0% average porosity, were used to change the subsonic boundary condition downstream of the interaction. Mass removal was variously concentrated toward the front or the rear of the holder. Porosity selection is determined by the desired pressure gradient, but is constrained by the requirements for obtaining a stable shock in the appropriate position within the flow time available in the Ludwig tube. The test time required for shock wave formation at the choking flap and its trajectory toward the holder lip depend significantly on total pressure, the ratio of total pressure to vacuum tank pressure, the porosity magnitude and distribution and the choke flap setting. Only a coarse range of choke settings was used with each porosity in the initial test, which was performed to explore subsonic boundary effects and to investigate the operational limits of the apparatus. As a result, only some of the porosity/choke setting combinations gave rise to stable shock patterns. All the combinations tested are recalled in Table IV, together with the character

of the shock structure obtained. The three combinations having stable bifurcations within the field of view of the schlieren at both $Re_L = 36 \times 10^6$ and 9×10^6 have been singled out for discussion. Measurements for the solid case ($\sigma = 0$), which gave a stable shock only at the lower Re_L are also presented.

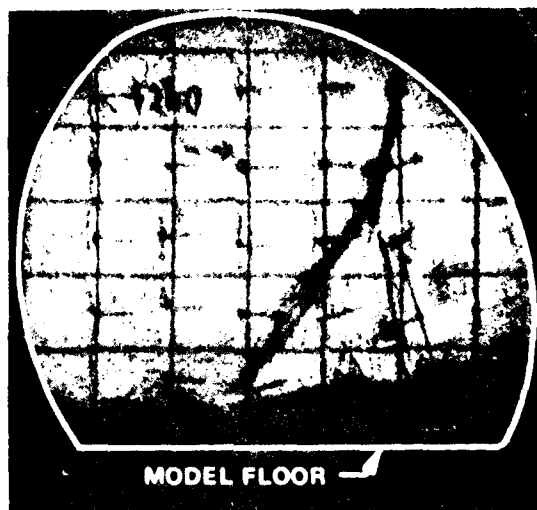
Table IV. CHARACTER OF THE SHOCK STRUCTURE OBSERVED WHEN CHANGING POROSITY/CHOKE SETTINGS.

POROSITY	$p_c = 138 \text{ KPa}$		$p_c = 35 \text{ KPa}$	
	$h_c \text{ (mm)}$	SHOCK	$h_c \text{ (mm)}$	SHOCK
0	308.9	MOVING	308.9	STABLE
	310.9			
	320.3			
2.2 AFT	308.9	MOVING	292.1	MOVING
	304.5			
	292.1			
4.6 AFT	292.1	STABLE	295.9	STABLE
	295.9			
	299.7			
6.7 DT	299.7	STABLE	299.7	STABLE
2.1 FWD	299.7	MOVING	-	-
9.4 LT	294.6	STABLE	299.7	STABLE
			301.0	
12.5	292.1	STABLE	-	-

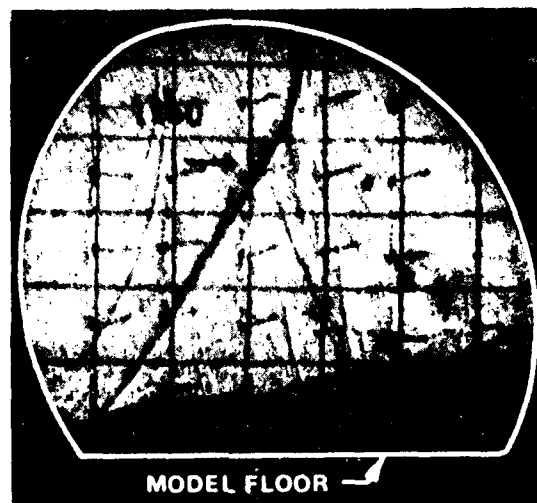
When the shock is stationary some distance ahead of the holder lip, the geometrical specification of the subsonic boundary is complicated by the flow spillage around the lip. The flow angle immediately behind the shock can be determined from the measured shock angle and Mach number to the extent that the shock is visible in the schlieren. Within the shock holder, the flow angle near the top wall (associated with flow through the top wall porosity) has been measured at a number of streamwise and lateral locations. These measurements are discussed in more detail in Section 3.7. The flow angle between the shock and the leading edge of the shock holder has not been measured, however, and that part of the subsonic boundary remains undetermined for cases in which the shock wave stands forward of the leading edge. Judging from the observation that the bifurcation height increases substantially when the shock moves forward of the shock holder lip, we assume that the average flow angle is larger in this region at the top plate height than it is within the shock holder. The flow angle immediately behind the shock at the maximum height visible in the schlieren (6 cm below the top plate), however, appears to be only about 4° compared with the leading edge flow angle of approximately 5° obtained by extrapolation forward from the probe measurements (see Section 3.7, Figure 22).

Extent of the Interaction

With all of the porous holder configurations tested, a well-defined shock structure was observed to move into the field-of-view at a speed between 10 and 20 ms^{-1} depending on the test parameters. A nearly normal upper wave branch and a tall bifurcated foot form the structure. Typically, the height of the bifurcation is observed to undergo minor changes as the upper normal shock travels within the model, Fig. 16A (and position "a" in the sketch of Fig. 17). The schlieren photographs in Fig. 16 show the deflection of boundary layer tufts which were mounted on the flow channel windows as a part of a concurrent corner flow investigation. They will not be discussed further here. Fig. 17 shows the variation in bifurcation height with distance along the flow channel for the porosities tested at $\text{Re}_L = 36 \times 10^6$. As the



(A)



(B)

Figure 16 OBSERVED SHOCK STRUCTURES, 9.4% LINEARLY TAPERED POROSITY

normal shock passes ahead of the holder lip, located at $X_e = 4.4$ cm, the forward movement of the bifurcation point is strongly reduced and its height increases rapidly, Fig. 16B (and position "c" in the sketch of Fig. 17). For the porosities that result in a stationary shock pattern, the height reaches a stationary value at that position which is indicated by the solid points in Fig. 17. It lasts until the end of the steady state test flow.

The stationary bifurcation heights of Fig. 17 cannot be correlated in a simple manner with the parameters that define the holder geometry since they depend upon the shock detachment distance. A similar situation was found in the analysis of the wall pressure distributions at this Reynolds number and in all the results at the lower Reynolds number as well. On the other hand, a qualitative correlation can be established, as expected, between the combined porosity and choke setting values and the position of the shock in front of the model. In Fig. 17, the bifurcation position is indicated by the abscissa X_λ of each solid point. The latter quantity can be approximately related to the detachment distance of the upper shock from the holder leading edge by inspection of the schlieren record. The detachment distance and the inclination of the upper shock can be assumed to control the flow angle and the amount of flow spillage at the holder lip. No significant variations in the inclination of the shock branches were detected at the different positions of the wave system.

On the basis of these observations, it was tentatively concluded that the interactions in front of the lip should correlate directly with the shock detachment distance, (or the related quantity $d_\lambda = |X_\lambda - X_e|$). This approach is taken in Table V and in the remaining description of the measurements.

Quantities that describe the vertical and streamwise extent of the interaction are listed in Table V versus decreasing distance (d_λ) of the bifurcation point from the holder leading edge. Their values are obtained from schlieren records and the surface pressures described in detail later.

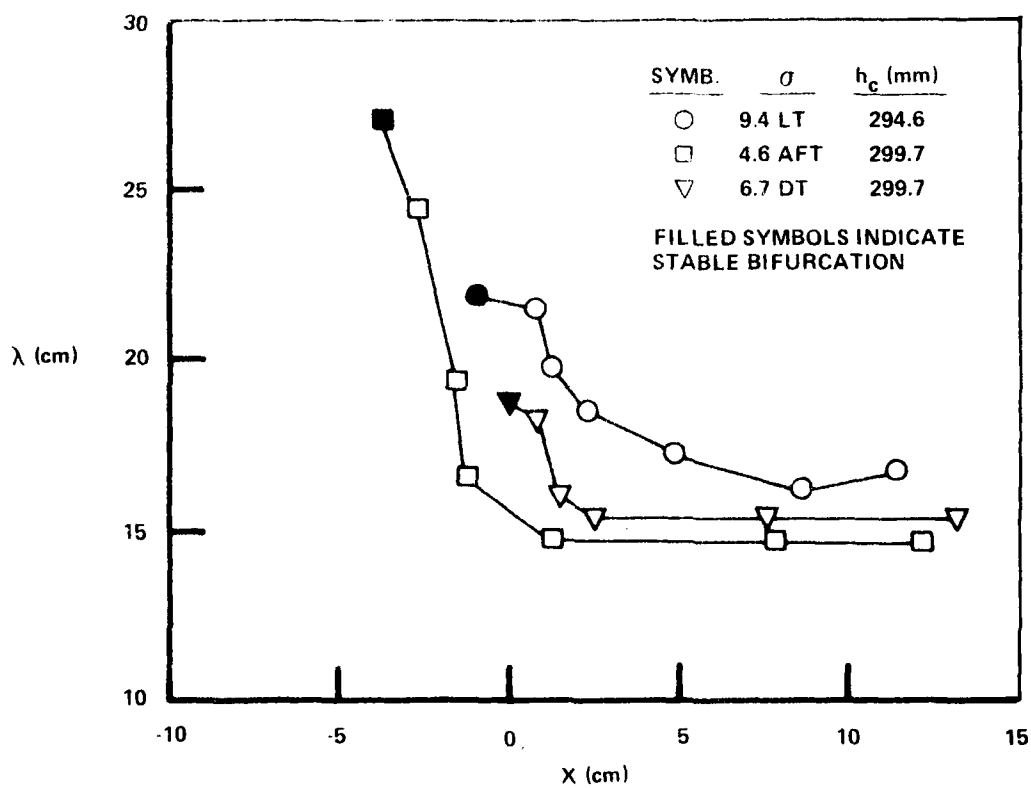
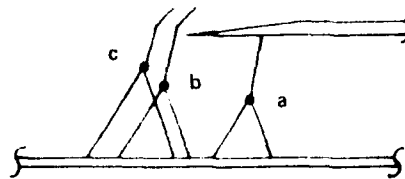


Figure 17 LOCATION OF BIFURCATION POINT, $M = 1.43$, $Re_L = 36 \times 10^6$

Table V. EXTENT OF THE INTERACTION VS. SHOCK POSITION.

$$Re_L = 36 \times 10^6; M = 1.43; \delta_u = 33.88 \text{ mm}$$

$d\lambda/\delta_u$	λ/δ_u	x_u/δ_u	$\frac{ x_k - x_u }{\delta_u}$
2.41	8.0	5.7	2.4
1.59	6.5	5.3	2.9
1.29	5.6	4.1	3.8

It is recalled here that x_u marks the beginning of the sharp linear pressure rise. Various experiments have shown that there is no ambiguity measuring from the surface pressure or from the shock pattern. The streamwise extent of the region of sharp pressure rise is given by $|x_k - x_u|$.

Table V emphasizes the findings of Fig. 17 by showing a reduction of about 40% in both the upstream and vertical extent of the interaction as the shock detachment distance is approximately halved. This is analogous to the interaction behavior observed for increases in Re_L . However, Table V indicates that when the bifurcation height is decreased by changes in the subsonic boundary of the interaction, the extent of the region of sharp pressure rise increases approximately 60%. This behavior is opposite to the Re_L one: halving of the bifurcation height by increasing Re_L reduced the region of sharp pressure rise by approximately 60% (Section 3.1, Table II). Other differences mark the reductions in the crosswise extent of interaction depending on whether they are obtained by increases in Re_L or by decreasing spillage. They will be pointed out in the discussion of wall pressures.

The preceding discussion is confined to measurements obtained with shock structures that were stationary in front of the holder lip. The data measured while the shock is moving through the shock holder flow channel strictly do not represent a steady flow case (as do the test points with the

shock located at its stable position ahead of the shock holder lip). However, the speed of the moving shock is small compared with the flow speed ($\approx 5\%$), and the trends from using moving shock measurements are believed to be correct and interesting.

The bifurcation heights observed while the shock is moving inside the holder do support the observation that a powerful factor in determining the extent of the interaction is the degree of constraint applied to the subsonic flow behind the shock. In Section 2.3, the variation along the shock holder length of the ratio of the critical cross flow per unit area to local mass flow per unit area W^*/W was given for each of the porosity distributions of Fig. 17. The correspondence between variations in W^*/W and stream tube area that exists within a 1D characterization of the flow was also noted. Figure 6 in Section 2.3 indicates moment differences in the rate of change in W^*/W near the lip for the three porosity distributions with the 9.4 LT porosity having the largest. Correspondingly, the bifurcation heights observed inside the holder fell in the range $\lambda/\delta_u = 1.4$ to 5, with variations small in comparison to those observed at locations in front of the lip.

In the 9.4 LT case, in which the local porosity increased to 12.5% as the shock moved forward, the increase in streamline deflection behind the shock contributed to a moderate continuing increase in the bifurcation height. For the other two porosities shown in Fig. 17, the porosity in the region $3 < X < 15$ cm was zero or nearly zero, and the λ height was smaller than that in the 9.4 LT case. Furthermore, because the porosity was not varying, no changes in flow deflection or constraint behind the interaction occurred, and the height remained approximately constant until the shock moved forward of the shock holder lip.

Wall pressures - During the investigation of the subsonic boundary effect, surface pressures were measured over the entire length of the model during each test. Pressure taps in the floor plate at fixed locations, more closely spaced at the lip, were used to this end. Additional measurements to fill in the basic coarse distribution were obtained when necessary by using

the moveable instrumented plate. Reading of pressure histories from each gauge at a fixed time produces a chronological description of the pressure rise in the model as the shock moves forward. Close to the lip, the shock is in the field of view and direct correlation of wall pressure and bifurcation extent is possible.

The two constant height bifurcation phases, described previously in relation to moving or stationary shocks, are found to have a precise correspondence in terms of surface pressures. When the bifurcation occurs inside the model, wall pressures are found to be very nearly self-similar in distance. Thus, the pressure level reached at any one fixed distance from the first rise is the same. As a result of the shock structure movement, however, the pressure at any fixed distance in the model frame of reference is continuously increasing. In particular, this is true at the outlet of the model, where a maximum in wall pressure is reached only when the shock structure is expelled from the lip. The effect of porosity during this phase has not been fully analyzed. It is apparent, however, that a relationship exists between the observed bifurcation height and the slope of the sharp pressure rise. This follows the trend observed previously in connection with Reynolds number increases: smaller bifurcation heights correspond to sharper pressure rises.

When the bifurcation occurs in front of the model, no further changes take place in the wall pressure inside the holder. The forward movement of the shock structure to its stable position is associated in this phase with a reduction of the kink pressure level, with the non-linear pressure rise following the kink describing an envelope line that matches the extrapolation of the pressure distribution inside the holder. Most remarkable is the insensitivity of the wall pressures to changes in the porosity distribution for all the interactions taking place in front of the lip. Fig. 18 shows the wall pressures recorded at a Re_L of 36×10^6 and a fixed time of 82 msec when each porosity/flap condition shown has reached its stable shock configuration. There is no detectable effect of the porosity on the pressure distribution region located inside the holder. Outside of it, the extent of the sharp

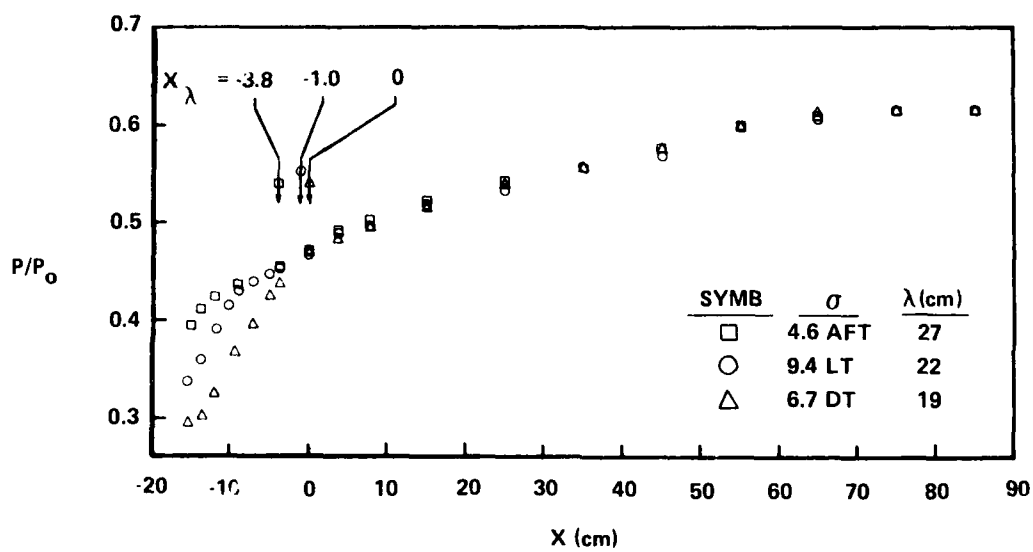


Figure 18 EFFECT OF SUBSONIC BOUNDARY VARIATION ON WALL PRESSURE, $Re_L = 36 \times 10^6$

pressure rise is reduced in proportion to the inverse of the bifurcation height. The locations of the observed bifurcation point are also recorded in Fig. 18. Their position, relative to the beginning of the sharp pressure rise, corresponds to a description of the shock structures as having constant inclination of the forward shock leg and the measured bifurcation heights.

Values of characteristic wall pressure parameters, obtained from Fig. 18, are summarized in Table VI for direct comparison with Table II of Section 3.1. The latter table described the observed Re_L influence on surface pressure. As already noted, both a decrease in flow spillage and an increase in Reynolds number produce a reduction in the height of the shock bifurcation. The flow events that bring about such an occurrence, however, must be quite different. This is suggested by differences in the trends of corresponding quantities in the two tables.

Table VI. WALL PRESSURE PARAMETERS VERSUS SHOCK POSITION.

$Re_L = 36 \times 10^6$; $M = 1.43$; Normal shock recovery = 0.668				
$d\lambda/\delta_u$	$\frac{\Delta(p/p_0)}{\Delta x}$	$(p/p_0)_k$	$x/\delta_u = 5$	$x/\delta_u = 10$
2.41	0.036*	0.415	78%	83%
1.59	0.036	0.43	78%	83%
1.29	0.037	0.45	78%	83%

* estimate, based on trend of available measurements and pre-stationary pressure distribution.

As the bifurcation detachment distance d_2/δ_u decreases and the bifurcation height drops from 8 to $5.6\delta_u$, the slope of the sharp pressure rise undergoes no change. Similarly, the recovery relative to normal shock reference level undergoes no change at the two control distances $x/\delta_u = 5$ and 10. In contrast, the kink pressure increases about 10%. A comparable percentage drop in bifurcation height from 5 to $2.7\delta_u$, obtained increasing Re_L from 9 to 36×10^6 , resulted in a more than twofold increase in the slope of the sharp pressure rise, about 10% increase in kink pressure and 12% increase in recovery at the upstream control distance.

Brief attempts to understand the above differences in terms of the known behaviors of the basic flow mechanisms of separation, reattachment, streamline deflection and curvature have not been successful. A thorough approach based on a complete mechanistic model and a flexible computational procedure appears to be required to explain the experimental results. In our judgment, this would represent the most valuable next step in the understanding of the transonic shock-boundary layer interaction.

Velocity profiles - Throughout the subsonic boundary investigation tests, velocity profiles were also measured at a fixed location situated toward the rear of the model at $X = 10.6$ cm. Rakes of various heights were used to this end. The tallest rake spans the entire model height with 10 static and 10 pitot probes.

In Fig. 19, velocity profile measurements, taken at distances from the shock holder floor ranging from 35 mm to 76 mm, are compared. They correspond to the variations in porosity discussed previously. In all cases, measurements at distances greater than 76 mm indicated u/u_s values of one. Measurements at distances smaller than 35 mm were only taken for $\sigma = 9.4$ LT due to the limited number of tests available. They confirm that zero velocity occurs essentially where indicated by the extrapolated line of Fig. 19.

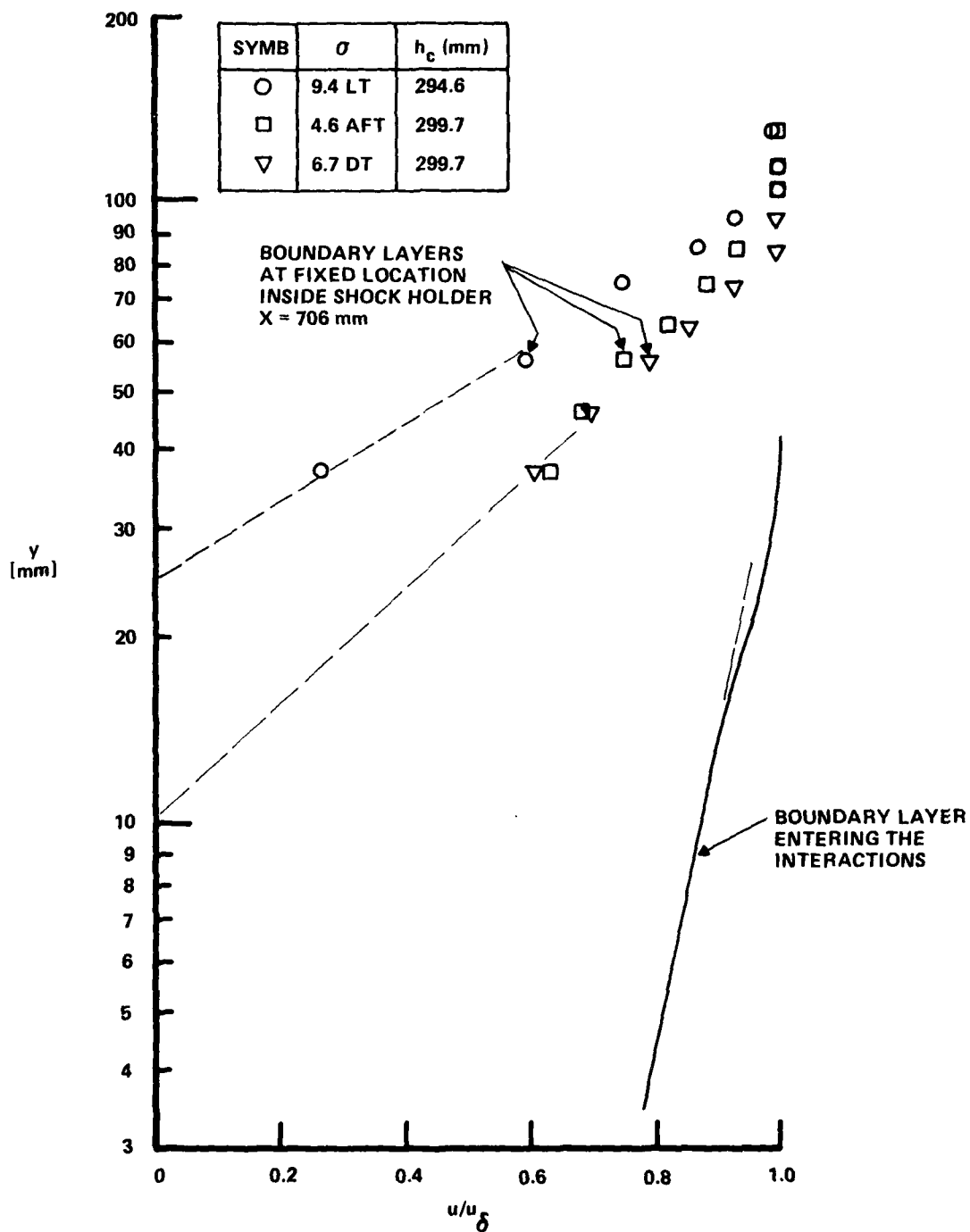


Figure 19 COMPARISON OF VELOCITY PROFILES

For all the stationary interactions generated with the porous shock holder, the velocity profiles indicate a dead air region near the model floor. Spot checks with the skin friction transducers at various downstream locations in the model concur to indicate that essentially zero friction occurs over a significant portion of the shock holder floor. An estimate of the vertical extent of the separated region is obtained from Fig. 19, using the criteria $u/u_s = 0$ and extrapolation. The velocity is 0 at 25%, 13%, and at less than 3% of the local viscous layer thickness, respectively for $\sigma = 9.4$ LT, 6.7 DT and 4.6 AFT. It is thus where the average porosity is the largest and concentrated forward that the region of separated flow is greatest at this location.

Further inspection of Fig. 19 reveals interesting details regarding the shape of the velocity profiles. First, as the shock is moved from the position closest to the shock holder lip, ($\sigma = 6.7$ DT) to a forward location ($\sigma = 9.4$ LT), the profile becomes less full. Its thickness increases from 76 to 100 mm with noticeable changes in the lower layer, as well as in the region of the wake component. This forward movement was obtained by closing the choking flap in excess of the amount required to compensate for the porosity opened up at the lip. An additional upstream displacement of the shock system was obtained by blocking completely the porosity at the holder lip. In this case, the choking flap was opened back to the value of the 6.7 DT case. The velocity profile in this case returned to a fuller distribution, analogous to the first observed. There are differences, however. The inner layer for the 4.6 AFT case shows velocities higher than the 6.7 DT velocities and the dead air region is confined to a few percent of the total thickness as already noted. In the outer layer, the opposite is true, the 4.6 AFT velocities are smaller than the 6.7 DT velocities. The thickness of the profile with the 4.6 AFT porosity has increased to approximately 100 mm.

Overall, Fig. 19 well illustrates the large readjustments in velocity distribution that accompany the changes induced in the shock bifurcation by varying its subsonic boundary. Too few measurements are available to formulate quantitative relationships. However, the existence of a marked

hierarchy in the degree of coupling of the subsonic pressure and velocity fields to their boundary constraints is well documented. In all the interactions, the wall pressure distribution became essentially insensitive to the shock structure and to the subsonic boundary at distances greater than $5 \delta_u$ behind the shock. In contrast, the velocity field is strongly affected up to a distance of $20 \delta_u$. Thus, at some distance from the shock system, it is with changes in the velocity distribution occurring at nearly invariant pressure that the flow manages to satisfy both a different history upstream and a change in downstream constraints.

3.6 Re_L Effect in Porous Shock Holder

A limited number of tests were devoted to generate interactions in the holder with the same porosities described in Sec. 3.2, but with the lower Re_L of 9×10^6 . Adjustments in choking flaps were found necessary in some cases to obtain a stationary shock pattern in the field of view within the available steady state test time.

Results of the test performed at $Re_L = 9 \times 10^6$ follow the same pattern described for the 36×10^6 tests. Both a constant height bifurcation slowly moving in the model and a constant height bifurcation stationary in front of the holder lip were observed. Figure 20 shows their values and locations. Comparing the values inside the holder, it is found that they have increased at equal porosity as the Re_L has decreased. The trend is similar to the one documented previously for the area relief shock holder. The λ increase due to the Re_L decrease is about 30% for the porosity distributions 9.4 LT and 6.7 DT, but only about 10% for the porosity of 4.6 AFT. Not enough information is available at this stage to interpret this result. For the shocks stationary in front of the lip, Fig. 21 shows again an increase of the vertical extent of the interaction as the distance of the shock in front of the lip increases.

Figure 21 presents wall pressures recorded at $Re_L = 9 \times 10^6$ with shock structures in the stable positions of Fig. 20. The observations made at the higher Re_L regarding the chronology of pressure development in the model, effect of position relative to the lip and effect of porosity remain valid.

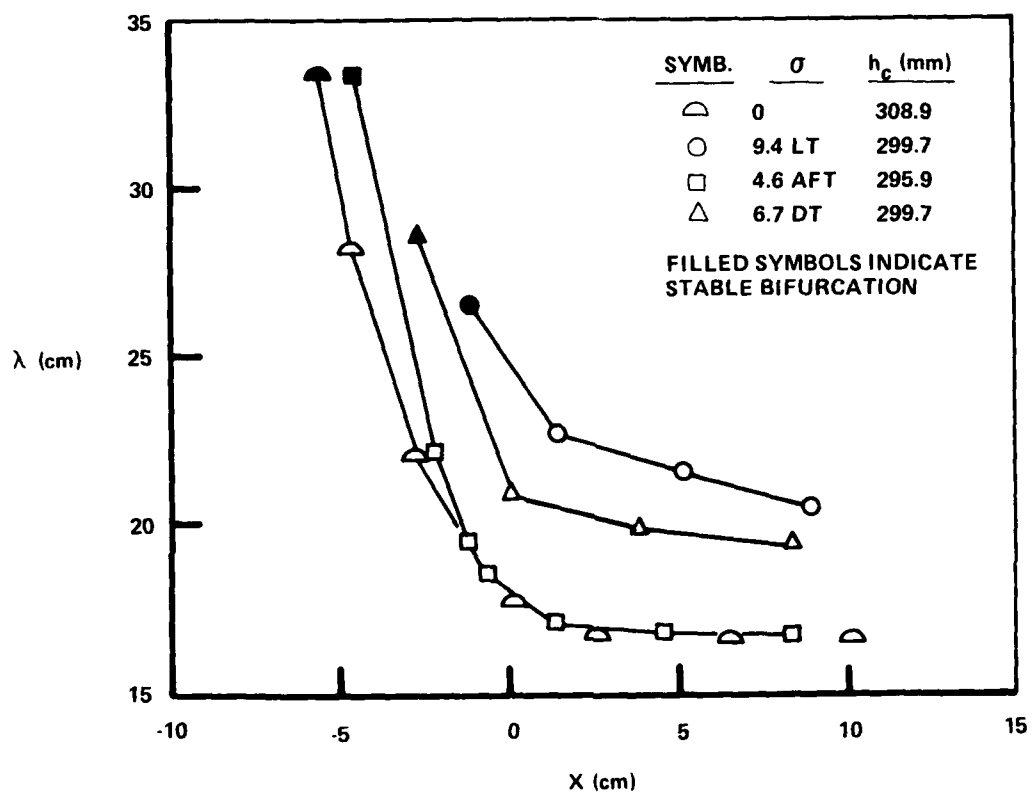


Figure 20 LOCATION OF BIFURCATION POINT, $M = 1.43$, $Re_L = 9 \times 10^6$

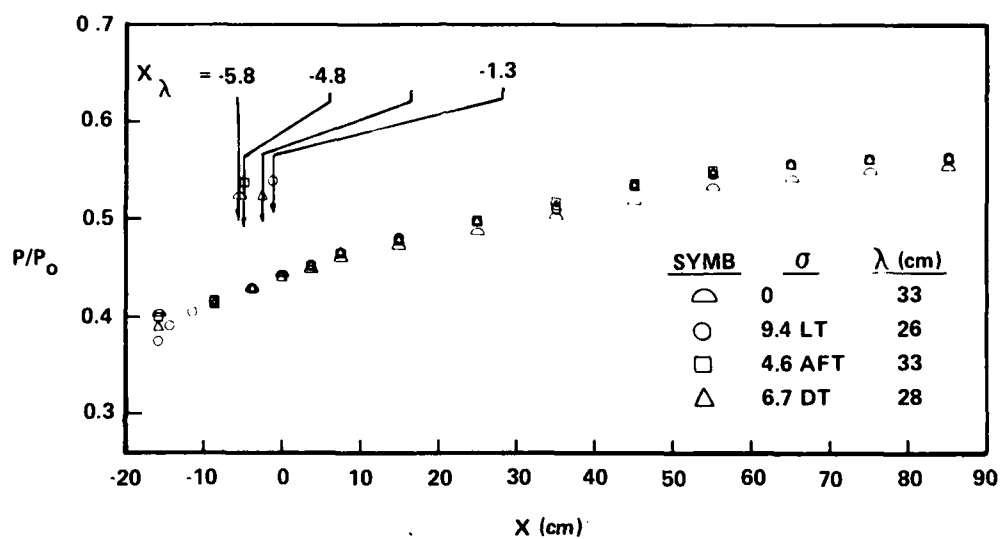


Figure 21 EFFECT OF SUBSONIC BOUNDARY VARIATIONS ON WALL PRESSURE, $Re_L = 9 \times 10^6$

However, at this Reynolds number, the sharp pressure rise falls beyond the limits of the deployed instrumentation. The wall pressure distribution inside the holder is somewhat lower for the zero porosity case than for the other porosities. Here there is no suction whatsoever applied to the boundary layer growing at the top surface of the holder and a larger viscous blockage effect is to be expected. Disregarding this difference, direct comparison of Figs. 18 and 21 shows a major effect of Re_L on the wall pressure in the interaction. The rate of pressure recovery is lower everywhere at $Re_L = 9 \times 10^6$, resulting in a level of 77.8% of the normal shock value at 35 cm behind the lip. This value compares with a corresponding 83.8% in the $Re_L = 36 \times 10^6$ results.

3.7 Additional Data for a Baseline Interaction.

Following the initial exploratory measurements, additional test runs were applied to describe details of the interaction that was obtained in the 9.4 LT model at $Re_L = 36 \times 10^6$. This was done to originate, in the porous shock holder, a data baseline case having flow field resolution comparable to that of the interactions obtained previously in the area relief holder. In addition, the flow angle near the top plate of the holder was measured during these tests. This completes the data set and should make it a particularly useful reference in future computation work.

Streamline deflections 3.8 cm below the porous holder surface were measured directly with the flow angle probe. The deflection measured was the pitch angle in the vertical plane of symmetry of the model. In general, the histories show a stable upward flow which is perturbed first by a large upward increment as the normal shock sweeps by and then subsides to a stable level larger than the undisturbed one. Streamline angles measured at three locations in the model are shown in Fig. 22. The open and filled symbols connected by a straight line represent flow deflections in the supersonic stream. They were measured both with a shock-free test flow (filled symbols) and in runs in which a shock was eventually established by using readings before the arrival

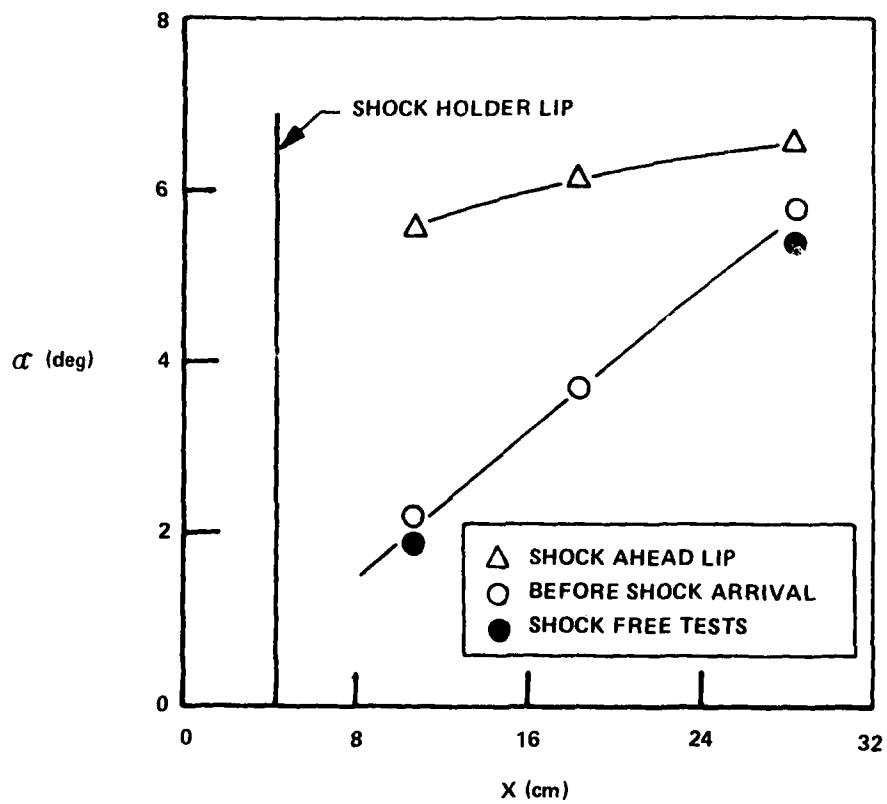


Figure 22 STREAMLINES ANGLE AT 9.4 LT SHOCK HOLDER, $Re_L = 36 \times 10^6$

of the shock. Regarding these measurements it should be noted that the probe was calibrated only at subsonic Mach numbers and the flow angles may not be accurate at supersonic speeds. The open triangles represent the flow deflections measured with the shock in the stationary position in front of the holder lip. The transient values associated with the passage of the shock at the probe were found to correspond well with the deflections estimated on the basis of local shock inclination as indicated by the schlieren record.

In addition to the flow angle measurements along the model centerline, the stream inclination was determined at a number of spanwise locations. This was done during the corner flow investigation²⁵ performed concurrently with the present work for the Office of Naval Research. Overall, the spanwise measurements support that description of the shock spanning the holder is essentially two-dimensional. The flow inclination is approximately 1.2° higher at 25 mm from the sidewall than at the centerline of the holder lip. This difference decreases downstream. At 100 mm from the model centerline, the top wall porosity is blocked by one of the strips used for its control. As expected, this introduces a local decrease in flow inclination. This is larger near the holder lip and decays downstream at the same rate as the difference between centerline and sidewall measurements. Use of more and narrower strips to block porosity would eliminate the latter spanwise non-uniformity, but this appears unnecessary for the study of the two-dimensional interaction that takes place in the neighborhood of the holder centerplane.

Skin friction at the floor of the model was measured directly with the minaturized balances at a number of streamwise locations. The length spanned is $-20 \text{ cm} < X < 20 \text{ cm}$, i.e. from just upstream of the shock system to well into the region of wall pressure insensitivity to subsonic boundary variations. The measurements are shown in Fig. 23. The skin friction with no shock in the holder is approximately constant at $C_f = 2.25 \times 10^{-3}$. When the shock is present, some skin friction disturbances occur upstream of the sharp dip in the C_f distribution. Separation, as defined by zero shear, is indicated at approximately $1.5 \delta_u$ upstream of the bifurcation point

25. Falk, T.J. and Padova, C., "Transonic Separation," ONR Project No. NR - 061-185 Quarterly Progress Report No. 4, March 1980.

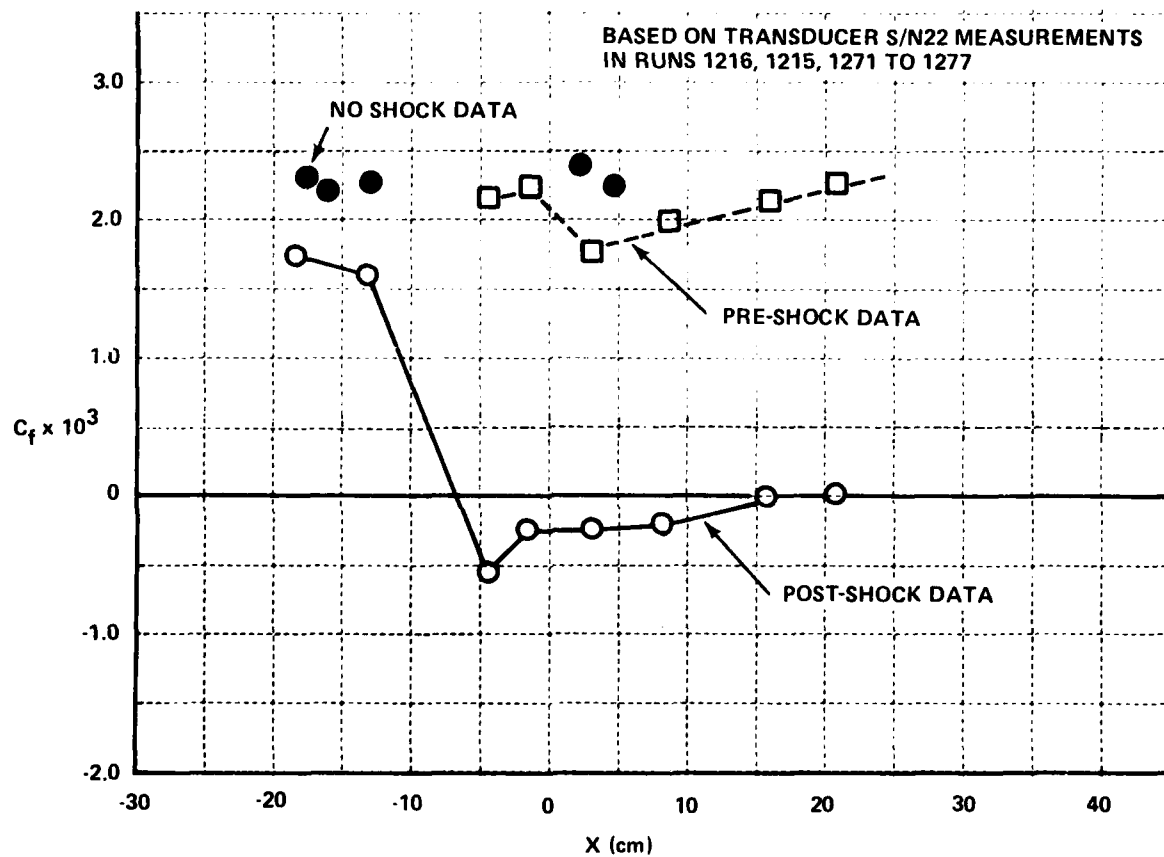


Figure 23 SKIN FRICTION DISTRIBUTION

location. This correlates well with the position of the kink pressure. As previously discussed in Section 3.1, this is a relevant feature of the interaction for which, unfortunately, contradictory measurements have been collected in the experiments available to this date. The negative skin friction values that occur in the region of separated flow are found to be only a small fraction of the undisturbed skin friction level. The minimum takes place somewhat upstream of the bifurcation point. Following it, the wall shear recovers to $C_f = 0$ approximately $6 \delta_u$ downstream, but it does not achieve positive values as far as the last available measurement location (velocity profile at $X = 20 \delta_u$). This feature distinguishes the interactions with mass removal downstream the shock from those obtained earlier in the area relief shock holder. A region of essentially stagnant air appears to remain at the floor of the holder for most of its length.

Velocity profiles at distances 1 and $20 \delta_u$ downstream of the bifurcation point were measured for the baseline interaction. They are compared in Fig. 24. The profile just downstream of the shock shows the characteristic velocity overshoot at vertical distances $40.6 < y < 76.2$ mm. The maximum speed corresponds to a Mach number 0.92 and occurs at $y/\delta_u = 1.4$. The velocity is zero at 18% of the typical viscous layer thickness (taken here at the location of the maximum speed). The profile far downstream indicates that the defect in momentum at the wall has diffused upward. The boundary layer thickness here is 101.6 mm and the zero velocity occurs at 25% of the local thickness. On the basis of the comparison of Fig. 24, it appears that, in the present shock-boundary layer interaction, the viscous displacement developing in the subsonic flow downstream of the shock did not undergo, during the rehabilitation phase, the characteristic decrease that was documented first by Seddon.

Of particular interest is the location of the maximum speed in the velocity profile at $X/\delta_u = 1$ in Fig. 24. The distance of the maximum from the floor is in fair agreement with the corresponding measurement at the same Reynolds number obtained with the area relief shock holder. The comparison

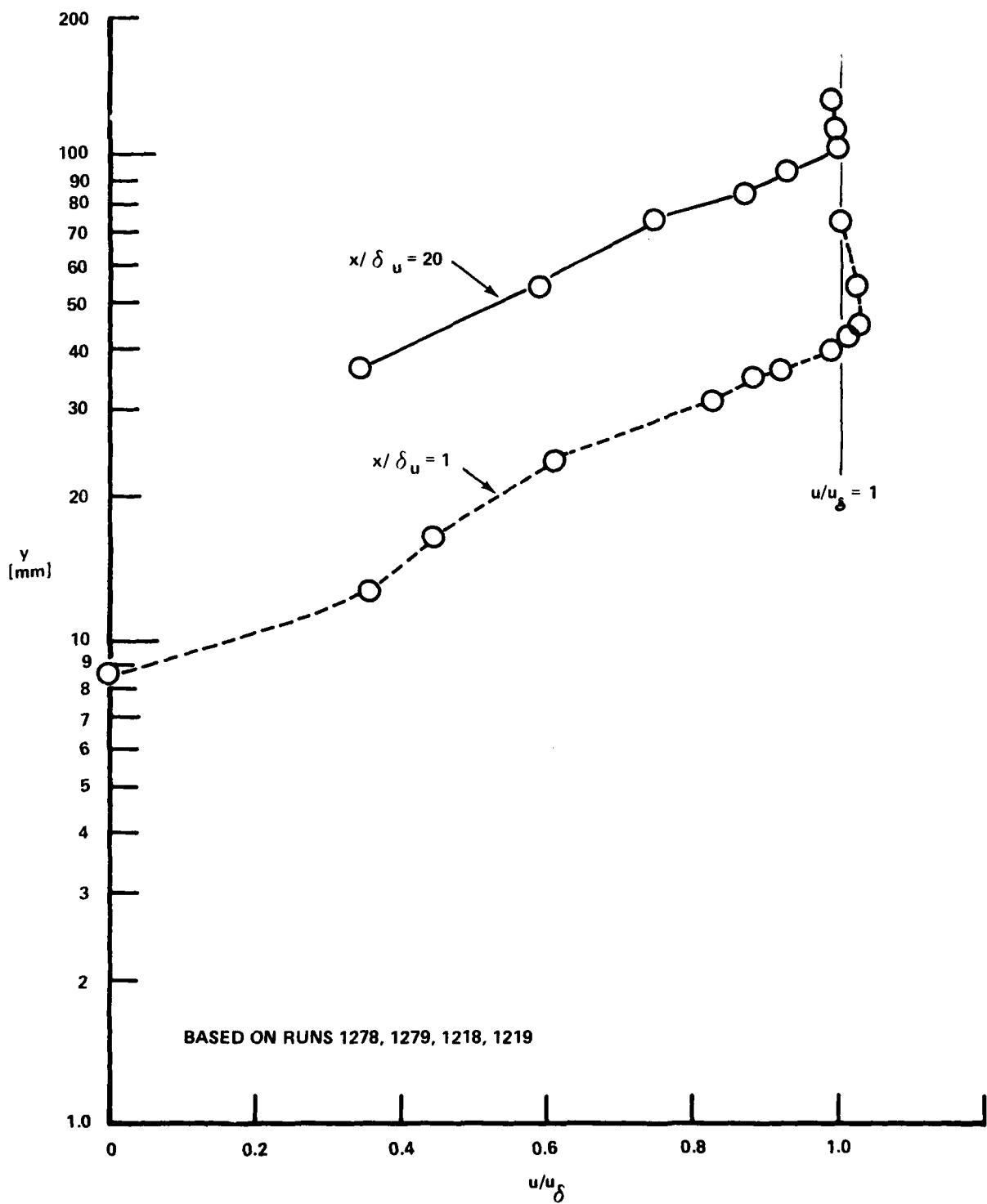


Figure 24 VELOCITY PROFILES AT 1 AND 20 δ_u

is only qualitative, because the available profiles in the two cases are not at the same streamwise location. However, there is good evidence that the location of the maximum speed scaled directly with δ_w and not with the bifurcation height at constant Re_L . This is different from the behavior observed when increases in bifurcation height were obtained by decreasing Reynolds number. It represents an additional manifestation of differences in the flow mechanisms that increase the extent of the transonic shock-boundary layer interactions in the two cases.

Section 4

COMPARISON WITH PREVIOUS EXPERIMENTS

The results of the present investigation reveal that transonic shock-boundary layer interactions are significantly affected by Reynolds number, Mach number, the ratio of wall-to-total temperature and, for the configuration tested, by the geometry of the subsonic flow boundary downstream of the interaction.

The distinctive feature of transonic shock-boundary layer interactions with flow separation is the shock bifurcation occurring at the wall. Seddon⁷, has described in detail the regimes that make up the total flow field. Based on examination of pressure distributions, velocity profiles and boundary layer integral parameters, the flow process within the viscous layer was found to consist of three phases. The shock phase, the displacement phase and the rehabilitation phase occur in sequence as the incoming viscous layer interacts with the shock system and progresses to a new equilibrium with the subsonic mainstream far behind the interaction. In addition to the basic interaction, studied in detail, Seddon reported tests with three modified interactions having different subsonic boundary geometries.

The heights of bifurcation observed in Seddon's basic interaction and in the experiments of Vidal et al³, Padova et al⁵, Kooi²⁰, East et al²¹, are compared in Fig. 25. The heights of bifurcation λ , normalized by δ_u , are plotted as a function of Reynolds number Re_{δ_u} . For each data point, the Mach number ahead of the shock and the wall-to-total temperature ratio are noted in parentheses. In all of these interactions, the ratio of viscous to mainstream flow satisfies the condition $\delta_u/h \leq 10\%$. Here h is the crosswise extent of the test flow that characterizes the inviscid mainstream in each experimental apparatus. Furthermore, all the interactions of Fig. 25 were obtained by choking the flow far downstream into the viscous rehabilitation region. Somewhat in analogy with Seddon's terminology, the inter-

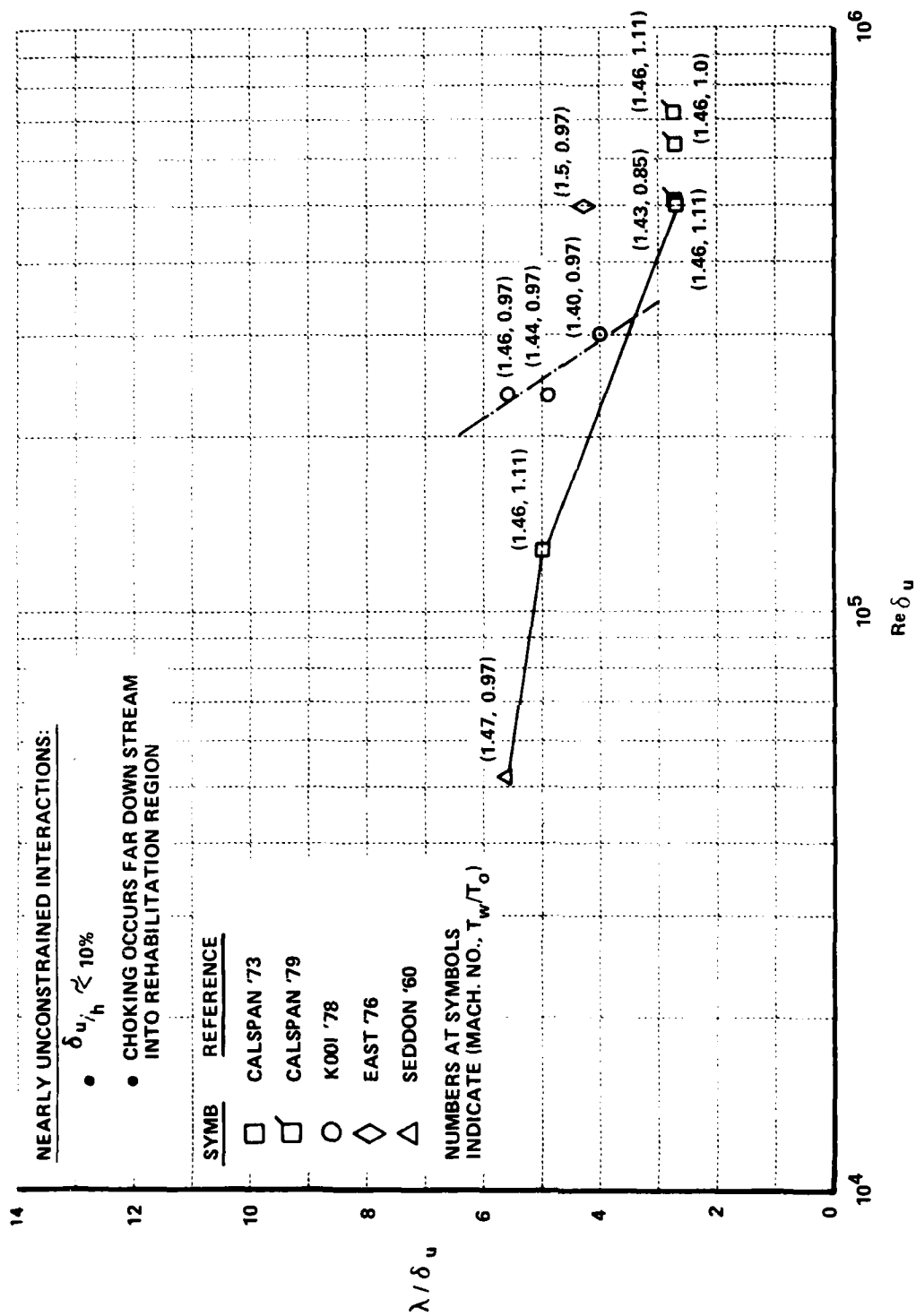


Figure 25 COMPARISON OF BIFURCATION HEIGHTS IN NEARLY UNCONSTRAINED INTERACTIONS

actions of Fig. 25 are labeled, "nearly unconstrained." In the Figure, Kooi's data at $Re_{\delta_u} = 2.3$ to 3.0×10^5 show the effect of Mach number on the height of bifurcation. A similar increase of the shock bifurcation height with increasing M was observed in Calspan data²² as recalled in Sec. 3.2. At constant M , the Calspan data at $Re_{\delta_u} = 1.3$ and 5×10^5 indicate how the bifurcation height decreases with increases in Reynolds number. From Fig. 25, the height of bifurcation is found to be insensitive to changes in temperature ratio within the range of values tested.

In Fig. 26, results from the present studies exploring boundary geometry effects on the interaction are compared with the trends of Fig. 25. The heights of bifurcation observed in Seddon's modified interactions are also included. All data points represent interactions that do not satisfy the second requirement set forth above for nearly unconstrained interactions. In all of these cases, the shock system was generated with a shock holder located close to the viscous displacement region. The ratios of viscous to mainstream flow range from 6 to 16%. However, in all cases, a shock bifurcation height of size comparable to h was observed and mass spillage at the lip of the shock holder was present. For each data point, the values of δ_u/h and $d\lambda/\delta_u$ are noted in parentheses. Here, $d\lambda$ is the streamwise distance of the bifurcation point from the shock holder lip. These interactions are termed "constrained."

Three interesting observations on how changes in the subsonic boundary geometry affect the interaction are derived from the comparison of Figs. 25 and 26. First, the threshold in the ratio of viscous to mainstream flow below which subsonic geometry changes affect λ negligibly, appears to fall between 5% and 10%. Seddon's basic interaction of Fig. 25 and the constrained one having $\lambda/\delta_u = 5.3$ in Fig. 26, both have $\delta_u/h \approx 6\%$, but differ widely in the position of the shock generator relative to the wave structure. Yet, an unaltered shock system is produced. Furthermore, detailed measurements in the constrained case show no changes in the surface pressure distribution up to well into the rehabilitation phase, where choking was imposed.

SYMB	REFERENCE	MACH NO.
◇	CALSPAN (PRESENT STUDIES)	1.43
△	SEDDON '60	1.47

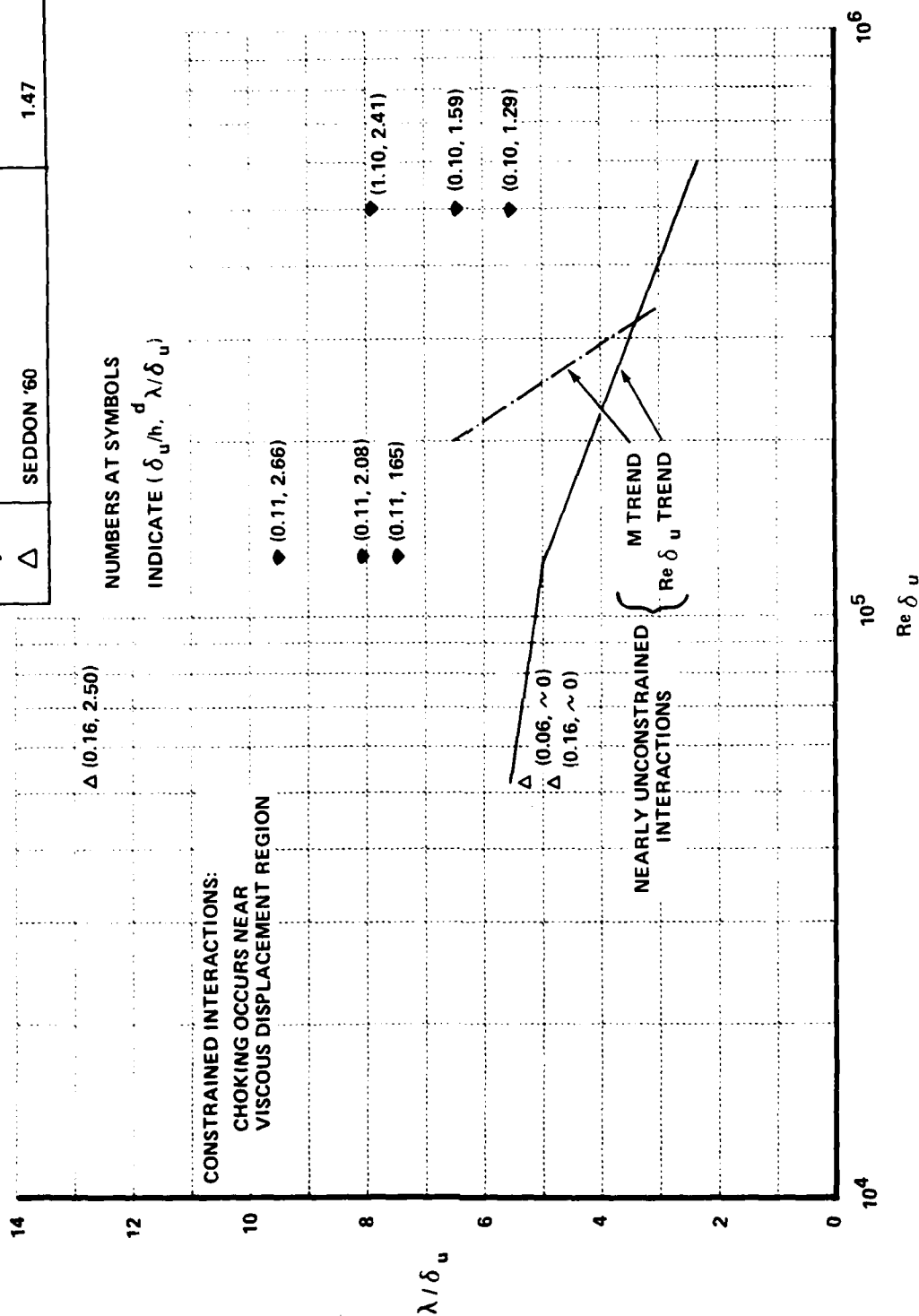


Figure 26 COMPARISON OF BIFURCATION HEIGHTS IN CONSTRAINED INTERACTIONS

However, several differences in the return to equilibrium of the velocity profiles were indeed observed. This emphasizes the fact that not all of the quantities describing the interaction are influenced to the same degree by constraintment.

Secondly, Seddon's data having $\lambda/\delta_u = 4.8$ in Fig. 27, indicates that with δ_u/h as high as 16%, it is still possible to tailor the subsonic boundary geometry so that the bifurcation height of the basic interaction is almost duplicated. This was obtained by adjusting the shock generator to provide a slightly divergent flow channel downstream of the interaction. No measurements, other than schlieren visualization were reported, thus nothing can be said regarding wall pressure and velocity profiles under the latter arrangement.

Thirdly, the data from the Calspan investigation of subsonic geometry at Re_{δ_u} of 1.3 and 5×10 (filled symbols in Fig. 27) show a sensitivity of the constrained interactions to Reynolds number changes that is similar to the one documented in the earlier studies. For these data, the correlation between the height of the bifurcation point and its streamwise distance from the holder lip has already been discussed. Its possible interpretation in terms of constraintment of the flow divergence in the displacement phase of the interaction was presented, as well. The Seddon data points at $\delta_u/h = 16\%$ in Fig. 27 confirm, qualitatively, both the Reynolds number trend and the correlation between λ and d_λ . The mapping of the plot domain is far from systematic because δ_u/h is significantly above the 10% of the Calspan data. Nevertheless, the range of bifurcation heights spanned by Seddon's data is compatible with that expected on the basis of the trends from the Calspan data, the increase in d_λ/δ_u and the decrease in Reynolds number.

Vidal et al³, Kooi^{16, 20}, and Mateer et al¹⁸ have shown the dependence of the surface pressure distribution on the Reynolds number ahead of the shock wave. In particular, Kooi¹⁶ compared his data obtained at $Re_L = 20 \times 10^6$ to Refs 3, 7 and observed that the initial pressure gradient

increases with increasing Reynolds number. The data of Mateer confirms this dependence. Later, Kooi²⁰ showed that the pressure distribution, after the initial rapid rise, is dependent on the Mach number ahead of the shock wave. The Calspan data⁴ show that the surface pressure distribution is independent of T_w/T_o when the streamwise distance is normalized by the undisturbed boundary layer thickness. The subsonic boundary condition investigation shows that the surface pressure distribution correlates directly with the height of the bifurcated shock structure. Variations in the constraints imposed on streamline deflections at the subsonic boundary result in changes in the height of the shock bifurcation. Taller bifurcations are found to correspond to smaller kink pressure values and to smaller slopes of the initial sharp pressure rise. However, changes in the subsonic boundary geometry that are imposed in the rehabilitation region do not influence the pressure recovery process.

The correlation between the changes in surface pressure near the shock and the height of bifurcation appears to hold in general. As pointed out, it is valid for increases in Re_L . This correlation also applies to the decrements in pressure which Kooi found occur with increases in M , which are associated with increases in λ . Kooi¹⁶ has shown that the pressure rise at the foot of the shock can be computed using a "free interaction" formula up to the point of impingement of the rear shock on the viscous layer. The formula used links $d\delta^*/dx$ to $M_\delta(x)$ via a Prandtl-Meyer compression model. The present results do not contradict such calculation scheme. However, they may restrict its applicability to a smaller distance at the shock foot.

Kooi²⁰ has compared the normalized separation length data of References 3,7,18,21 and 27. The Calspan data used in that comparison were taken at $T_w/T_o = 1.11$ and 1.0 (Refs. 3, 28), and Kooi did not note the dependence of normalized separation length on the temperature ratio. Kooi's comparison suggests that both the Mach number and Reynolds number have a strong influence on the extent of separation. The normalized separation

length increases with increasing Mach number and decreases with increasing Reynolds number.

A comparison of normalized separation length as a function of Reynolds number Re_{δ_u} , similar to that made by Kooi, is shown in Fig. 27. Data obtained in References 7, 20, 21, 27 and 28 are compared with previous Calspan data and with present results. For each data point, the Mach number ahead of the shock and the temperature ratio T_w/T_o are noted in parentheses. As indicated above, Kooi's data at $Re_{\delta_u} = 2.3$ to 3.0×10^5 , shows the effect of Mach number on separation in that the separation length increases with Mach number, while the previous Calspan data at $M = 1.43$ and $T_w/T_o = 1.11$ and Kooi's data at $M = 1.44$ and $T_w/T_o = 0.97$, show that separation length decreases with increasing Reynolds number. In Fig. 27, the Calspan data at Reynolds numbers from 5×10^5 and 7×10^5 illustrate the trend of increasing separation length with decreasing temperature ratio.

The results of the subsonic boundary investigation correspond to Re_{δ_u} values of 5×10^5 and 1.3×10^5 , at which separation lengths in excess of 20 occur. On the basis of all of these data, it appears that separation length is much more sensitive to Mach number and temperature ratio and flow constraintment than to Reynolds number.

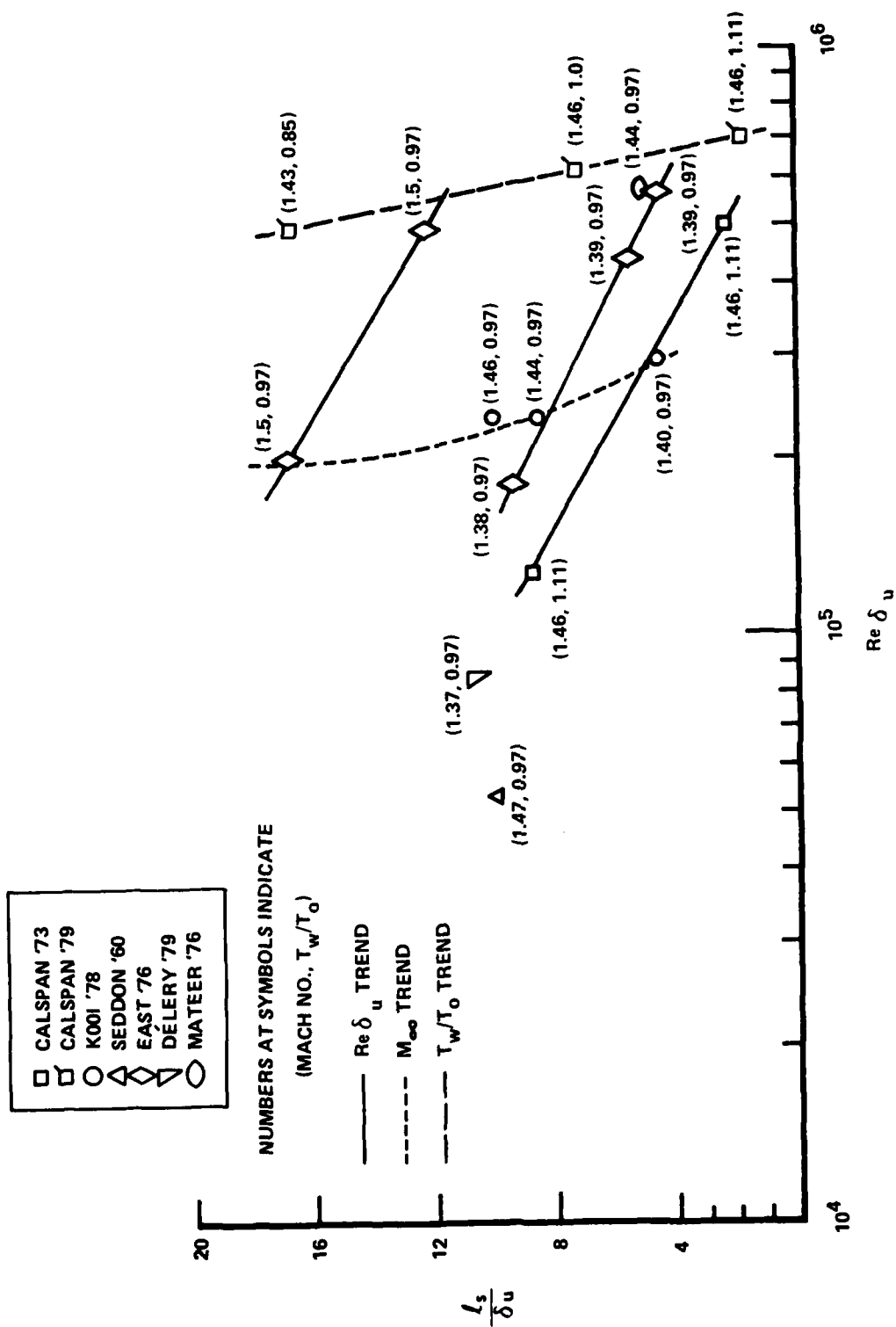


Figure 27 COMPARISON OF SEPARATION LENGTH MEASUREMENTS

Section 5

CONCLUSIONS

Interactions of a normal shock with a turbulent boundary layer have been investigated experimentally at Re_L from 9×10^6 to 72×10^6 , unit Reynolds numbers 14.8×10^6 and $29.5 \times 10^6 \text{ ft}^{-1}$, Mach numbers 1.43 and 1.60, and wall-to-total temperature ratios from 0.85 to 1.11. In addition, the effect of changing the subsonic boundary condition downstream of the interaction has been explored by using various amounts of porosity in the shock generator sustaining the shocked flow. The analysis of the data has led to the following conclusions.

(A) With regard to the characteristic length scales of the interaction:

1. The normalized height of the bifurcated shock structure, decreases with increasing Reynolds number at fixed boundary condition. It depends remarkably on constraints imposed on the deflection of the flow downstream of the interaction, when the ratio of viscous to mainstream flow is 10% or greater. It does not depend on the wall-to-total temperature ratio in the limited range of values investigated. The bifurcation height increases with increasing Mach number and is more sensitive to M than to Reynolds number variation.
2. The normalized length l_s/δ_u of the separated flow region is found to decrease as the wall-to-total temperature ratio is increased. Reduction in the extent of separation behind the shock was obtained in past experiments by decreasing Mach number or by increasing the Reynolds number of the incoming flow. The length of separated flow region responds dramatically to the moderate but sustained flow deflections imposed by the perforated shock holders that were tested. No reattachment occurred in the present exploratory tests over a distance of over 20 undisturbed boundary layer thicknesses downstream of the interaction. Aggregate results from four applicable investigations of the variations of l_s/δ_u

are still insufficient for an empirical formulation of the functional dependence of separation length on Re_{δ_u} , M and T_w/T_o . However, the stated trends are well defined. Furthermore, it is found that l_s/δ_u is much more sensitive to variations in Mach number wall-to-total temperature ratio and subsonic flow constraint than to Reynolds number.

3. A basic difficulty arises in the definition of the extent of the interaction. There exists a marked hierarchy in the degree of coupling of the subsonic pressure and velocity fields to the conditions defining the interaction. The wall pressure distribution becomes essentially insensitive to the shock structure and the subsonic boundary conditions at distances of a few undisturbed boundary layer thicknesses behind the shock. This is not true for the velocity field. At some distance from the shock system, it is with changes in the velocity distribution occurring at nearly invariant pressure that the flow accommodates variations in the conditions defining the interaction. Correspondingly, inferences on shock-boundary layer interactions based on surface pressure measurements only, which are frequently drawn in airfoil work, appear questionable.

(B) With regard to surface pressure distributions:

1. In general, the surface pressure distribution is found to correlate directly with the height λ of the bifurcated shock structure. Steep linear pressure rises to higher kink pressure levels are associated with small λ and vice versa. The coupling of the surface pressure distribution with the shock structure dies out quickly in the displacement phase of the boundary layer development. The effects of M , Re_L and the subsonic boundary conditions on the bifurcation height are, thus, reflected essentially in the initial region of the surface pressure distribution.

2. The surface pressure distribution has been found to be independent of wall-to-total temperature ratio when heat transfer effects on the incoming boundary layer are accounted for in the definition of the interaction boundary conditions (i.e., when streamwise distance is normalized by the undisturbed boundary layer thickness δ_u).

3. There appear to be differences in the manner in which the wall pressure responds to bifurcation height changes, depending on whether these changes are obtained at constant or varying Re_L . Higher kink pressures obtained by increases in Re_L are accompanied by steepening of the initial pressure rise. In addition, higher pressures occur up to distances $10 \delta_u$ downstream the shock. In contrast, higher kink pressures obtained at constant Re_L by reducing the subsonic flow constraint are accompanied by no change in the slope of the sharp pressure rise. Essentially, equal pressures occur as early as $5 \delta_u$ downstream of the interaction.

(C) With regard to surface skin friction:

1. Surface skin friction measurements, using flush-mounted transducers, were used to determine the onset of boundary layer separation and reattachment. The onset of separation, relative to the location of the normal shock wave, was found to move downstream with increases in Re_L , but it is independent of the temperature ratio, T_w/T_o . The large changes in the length of the separated flow region are due to large movements of the reattachment point. Reattachment occurs farther upstream of the normal shock as the Re_L is increased and farther downstream as T_w/T_o decreases.

REFERENCES

1. Loving, D.L., "Wind-Tunnel-Flight Correlation of Shock-Induced Separated Flows," NASA-TN-D-3850, September 1966.
2. Pearcey, H.H., Osborne, J. and Haines, A.B., "The Interaction Between Local Effects at the Shock and Rear Separation - A Source of Significant Scale Effects in Wind-Tunnel Tests on Aerofoils and Wings," AGARD Conference Proceedings No. 35, Paper No. 11, 1968.
3. Vidal, R.J., Wittliff, C.E., Catlin, P.A. and Sheen, B.H., "Reynolds Number Effects on the Shock Wave-Turbulent Boundary-Layer Interaction at Transonic Speeds," AIAA Paper No. 73-661, AIAA 6th Fluid and Plasma Dynamic Conference, Palm Springs, CA, 16-18 July 1973.
4. Padova, C., Falk, T.J. and Wittliff, C.E., "Experimental Investigation of Similitude Parameters Governing Transonic Shock-Boundary Layer Interactions," AIAA Paper No. 80-0158, AIAA 8th Aerospace Sciences Meeting, Pasadena, CA, 14-16 January 1980.
5. Padova, C. and Wittliff, C.E., "The Effects of Wall-to-Total Temperature Ratio on Shock Wave-Turbulent Boundary Layer Interactions at Transonic Speeds," Calspan Report No. WF-6091-A-1, October 1979.
6. Sheeran, W.J. and Hendershot, K.C., "A New Concept of a Variable-Mach Number Perforated Wall Nozzle for Providing a Supersonic External Stream in Rocket-Propulsion Testing," AIAA Paper 68-238, March 1968.
7. Seddon, J., "The Flow Produced by Interaction of a Turbulent Boundary Layer with a Normal Shock Wave of Strength Sufficient to Cause Separation," ARC R&M No. 3502, March 1960.
8. Davies, W.R. and Bernstein, L., "Heat Transfer and Transition to Turbulence in the Shock-Induced Boundary Layer on a Semi-Infinite Heat Plate," J. Fluid Mech., Vol. 36, Pt. 1, pp 87-112, 1969.
9. Bogdan, L., "Instrumentation Techniques for Short-Duration Test Facilities," Calspan Report No. WTH-030, March 1967.
10. MacArthur, R.C., "Contoured Skin Friction Transducers," Calspan Report No. AN-2403-Y-1, August 1967.
11. Wittliff, C.E., Pflueger, P.G. and Donovan, P.J., "A High-Speed Digital Data Acquisition System For Short-Duration Test Facilities," International Congress on Instrumentation in Aerospace Simulation Facilities, Monterey, CA, 24-26 September 1979.

REFERENCES (cont'd.)

12. Adcock, J.B., Peterson, J.B. and McRee, D.I., "Experimental Investigation of a Turbulent Boundary Layer at Mach 6, High Reynolds Number and Zero Heat Transfer," NASA TN D-2907, July 1965.
13. Winter, K.G. and Gaudet, L., "Turbulent Boundary-Layer Studies at High Reynolds Numbers at Mach Numbers Between 0.2 and 2.8," R.A.E. RM No. 3712, December 1970.
14. Mabey, D.G. and Sawyer, W.G., "Experimental Studies of the Boundary Layer on a Flat Plate at Mach Numbers from 2.5 to 4.5," R.A.E. RM No. 3784, September 1974.
15. Wittliff, C.E. and Vidal, R.J., "Transonic Separation," ONR Project No. NR 061-18519-4-70 (438) Annual Progress Rept., December 1973.
16. Kooi, J.W., "Experiment on Transonic Shock-Wave Boundary Layer Interaction," AGARD CP-168 (also, NLR MP 75002 U), 1975.
17. Little, B.H., "Effects of Initial Turbulent Boundary Layer on Shock-Induced Separation in Transonic Flow," von Karman Institute for Fl. Dyn., Tech. Note 39, October 1967.
18. Mateer, G.G., Brosh, A. and Viegas, J.R., "A Normal Shock-Wave Turbulent Boundary-Layer Interaction at Transonic Speeds," AIAA Paper No. 76-161 presented at the AIAA 14th Aerospace Sciences Meeting held in Washington, D.C., January 26-28, 1976.
19. Vidal, R.J., "Wall Interference Effects in Transonic Flow," OSR Contract No. F44620-71-C-0046, Annual Inventory of Research, September 1972.
20. Kooi, J.W., "Influence of Free-Stream Mach Number on Transonic Shock-Wave Boundary-Layer Interaction," NLR MP 78013 U, 23 May 1978.
21. East, L.F., "The Application of a Laser Anemometer to the Investigation of Shock-Wave Boundary-Layer Interactions," AGARD CP-193, May 1976.
22. Vidal, R.J., "Transonic Shock-Wave-Boundary Layer Interactions," Calspan Report No. AB-5866-A-2, August 1978.
23. Vaglio-Laurin, R., "Studies of Separated Flows," Final Scientific Report Grant No. AFOSR-72-2316, New York University Division of Applied Science, Unpublished. September 1974.
24. Falk, T.J. and Padova, C., "Transonic Shock-Wave-Boundary Layer Interactions," Calspan Report No. AB-5866-A-3, March 1979.

REFERENCES (cont'd.)

25. Falk, T.J. and Padova, C., "Transonic Separation," ONR Project No. NR 061-185 Quarterly Progress Report No. 4, March 1980.
26. Sawyer, W.G., East, L.F. and Nash, C.R., "A Preliminary Study of Normal Shock-Wave Turbulent Boundary-Layer Interactions," RAE Tech. Memo 1714, June 1977.
27. Vidal, R.J. and Catlin, P.A., "Investigations of Shock Wave-Turbulent Boundary-Layer Interactions at Transonic Speeds," Calspan Report No. WF-5746-A-1, April 1977.
28. Délery, J. and Le Dinzet, P. "Décollement Résultant d'une Interaction Onde de Choc/Couche Limite Turbulente," ONERA T. P. No. 1979-146, XVI Colloque d'Aérodynamique Appliquée (AAAF), Lille, 13-15 Novembre 1979.